THE ROLE OF HYBRID SYSTEMS IN THE DECARBONIZATION OF RESIDENTIAL HERITAGE BUILDINGS IN MEDITERRANEAN CLIMATE. A CASE STUDY IN SEVILLE, SPAIN.

Abstract.

Residential heritage buildings in the Mediterranean region face unexpected challenges in the field of energy efficiency and indoor environmental quality to ensure the sustainable conservation of historic town centres. This paper evaluates whether the conservation of their values can coexist with the current energy efficiency requirements and be included in urban decarbonization plans to prevent neglect and degradation. For this, a comprehensive decarbonization plan was drawn up based on the results of a previous energy audit on the case study selected, an 18th-century listed residential building in Seville, Spain. Envelope improvement was combined with mechanical ventilation and an integrated heat pump combining RESs and electricity from the public grid to cover all thermal needs in order to reach NZEB performance in the building. Despite the complexity of integrating demanding energy efficiency standards into heritage buildings, which requires case-by-case analysis and dynamic simulation, findings show a notable degree of approximation to NZEB performance. The main obstacles stem from the large amount of energy consumed by auxiliary systems and the relatively low presence of RESs in the national electricity mix.

Key words

Heritage housing; Built heritage decarbonization; Energy retrofit; RES building integration; Hybrid energy system; Thermal comfort.

Abbreviations

ASHP: air-source heat pump;

ASrHP: air-to-water reversible heat pump;

DHW: domestic hot water;

EWH: electric water heater;

FE: final energy (kWh);

GHG: greenhouse gases;

HP: heat pump;

IAT: indoor air temperature (℃);

IAQ: indoor Air Quality;

MVS: Mechanical ventilation system;

NEC: Spanish national energy code;

NZEB: near-zero energy building; nrPE: non-renewable primary energy (kWh);

n50: air change rate at 50 Pa (h^{-1});

OAT: outdoor air temperature (℃);

OHD: occupied hours of discomfort (h);

PE: primary energy (kWh);

PEF: primary energy factor (dimensionless);

PEG: public electricity grid;

PV: photovoltaics;

RES: renewable energy sources;

SPF: seasonal performance factor (dimensionless);

TC: thermal comfort;

U-value: thermal transmittance (W/m^2K).

1. Introduction.

Since 2012, energy efficiency requirements in building renovation have been mandatory for all EU buildings, except those listed for their heritage values [1]. There is now widespread consensus on the adverse effects that such an exception may entail, as it is thought that it could encourage abandonment and prevent ambitious EU decarbonization targets from being met [2]. In social terms it is also unfair to the population living in conservation areas, who are left more vulnerable to risks arising from energy obsolescence and climate change, in contradiction with the heritage conservation principles proclaimed by UNESCO [3] and ICOMOS [4,5] under the new sustainability approach. In view of this, in the last decade this issue has become the focus of a significant number of EU-funded projects [6–10].

It is true that the energy retrofit of heritage buildings is a challenging multi-objective task, often described as a balancing procedure, which requires trade-offs between conflicting goals [11] of different types: conservation (preservation of the integrity of the constructive elements, the historic urban landscape and the archaeological remains); economy (cost-effectiveness and economic feasibility); environment (GHG emissions during the buildings' operational stage and impact of materials and processes during their whole life cycle); and health (thermal comfort and indoor air quality (IAQ)). The need to bring together all these targets has recently become an additional incentive for the standardization of the decision-making process [12], [13]. One of the more complex tasks is that of cutting the levels of primary energy consumption of fossil fuel down to those set for non-listed buildings, something which necessarily involves the integration of renewable energy sources (RESs) in their energy supply, usually hindered by regional and/or local heritage conservation policies. Some of these policies are applicable at building level, protecting the constructive integrity and authenticity of the envelopes, while others are designed to prevent visual pollution (hindering the installation of RESs based on solar collectors such as PV or solar thermal) or to safeguard the archaeological remains within the conservation areas (impeding the implementation of geothermal technologies, although these are excellent solutions when coupled with other hybrid systems in warm climates [14], [15]).

Historic buildings make up almost a quarter of European building stock [16],[17]. It is estimated that 13.1% of the existing residential buildings in Spain were built before 1945 [18], limit date for a building to be considered as "historic" [17] . Unfortunately, there are no statistics on the exact number of listed buildings neither in Spain nor in Andalucía and therefore, their energy impact on the total stock cannot be calculated at present. Since the beginning of the 1980s, public policies for the protection of the urban heritage have increasingly included a larger fraction of residential buildings in the protection catalogues. Thus, the vast majority of this 13.1% is made up of buildings affected by specific

protection rules according to their assigned value or are located in neighbourhoods with strong historic urban identity where special landscape protection rules apply.

The aim of this paper is to establish the extent of the potential decarbonization (i.e. reduction in fossil-fuel energy consumption and CO_2 emissions) of historic housing in the EU Mediterranean region, while improving thermal comfort and IAQ in the dwellings in compliance with heritage protection regulation. For this, we use an 18th-century residential listed building located in the conservation area of Seville, Spain, as a reference for simulations, analysing the combined effect of RES integration and the application of the commonly adopted package of energy measures.

In the Mediterranean region, with its rich and diverse built heritage, recent research has often mainly focused on the conservation and energy savings of individual public buildings of outstanding heritage value [19–23]. While their abundance makes them key players in urban decarbonization strategies, less attention has been paid to heritage housing (despite health implications), which is mostly low-grade listed [24–28]. Success is dependent on the use of a further-reaching strategy which, in addition to carrying out the energy retrofit of a few unique buildings, should also consider this large stock of historic housing, attempting to ensure maximum compatibility with energy efficiency in order to ensure its continued use. Seville, which holds one of the most populated and extensive conservation areas in Europe, with the highest level of national protection, is a particularly appropriate study territory for experimentation on these strategies.

As in the rest of the EU [29] most housing energy consumption in the Spanish Mediterranean region comes from thermal facilities: heating, cooling, and domestic hot water (DHW) production account for 61% of the total final energy (FE) consumed in blocks of flats [30]. In addition, energy supply is largely provided by fossil-fuel sources (42% public electricity grid (PEG) and 38.4% liquefied petroleum gas, diesel, and natural gas) while only 1.6% derives from solar-thermal and geothermal sources. Therefore, the achievement of the ambitious EU 2030 building-decarbonization targets in the EU Mediterranean region would require a threefold strategy: (1) lowering the FE consumed by the thermal facilities of dwellings, while improving indoor environmental conditions; (2) increasing the share of RESs produced on site or nearby; and (3) increasing the share of RESs involved in PEG generation. These goals are more difficult to meet in the energy retrofit of heritage buildings. Firstly, heritage conservation rules severely limit the potential improvement of the thermal transmittance (U-value) of the envelopes, hampering large reductions in heating and cooling demand and thus in the FE consumed for thermal conditioning of dwellings. In practice, the energy retrofit of heritage housing in the Spanish Mediterranean region is mostly limited to the replacement of windows and thermal insulation of roofs. However, this is not enough to bring them in line with the current EU energy efficiency standards applicable to non-listed buildings and, furthermore, it may adversely affect the IAQ of the dwellings [31–33]. When comfort and health variables are considered, the use of traditional

mechanical systems for air conditioning and/or ventilation intensifies and the FE consumption usually rockets. Secondly, the integration of RESs on site or nearby is not only hindered by regulatory issues, as previously mentioned, but also by practical problems: dense urban areas, such as those of the Mediterranean historic city centres, display a limited potential for solar system applications as the roof area available in multi-family buildings rarely exceeds 40% [34]. This is due to shading issues or conflicts with the intense use of flat roofs as recreational private space as their surface, which is generally limited, has to be shared with facilities including stairs and elevator shafts, perimeter safety areas, storage rooms, antennas and air conditioning devices. Similarly, the ground space needed for heat exchangers of geothermal solutions is usually also not available in these compact historic city centres. In contrast, the third goal, the increase in the renewable share in national electricity mixes, is increasing worldwide, reaching almost 27% in 2019 according to an IEA Tracking report [35]. In Spain, low-carbon sources (renewables and nuclear) accounted for 43.6% of all electricity produced in 2020, their highest share in the generation mix since records began in 2007 [36].

This progressively lower carbon PEG boosts the implementation of flexible energy *hybrid systems*, capable of combining RESs with electrically driven highly efficient devices. A variety of hybrid energy solutions, currently available for building applications, appear promising in the decarbonization of residential buildings in the Mediterranean region [37], [38]. One of the more developed hybrid technologies is based on electrically driven heat pumps (HPs which require lower electric input energy than the output energy they produce. In the context of a low-carbon PEG this pushes the reduction of primary energy consumption and CO_2 emissions. HP performances and efficiencies have increased considerably over the past 30 years, largely thanks to better system integration and new technologies and components. Both these factors have fostered research on the topic [39–43]. The most common is the air-source HP (ASHP) which produces energy on site, using freely available and renewable ambient heat, found everywhere at a relatively low cost and with an excellent performance at part loads [44], [45]. ASHPs are particularly well suited to heritage housing retrofits thanks to the minimal space required, easy installation, and compatibility with archaeological and landscape protection regulations. The portion of RESs used by an ASHP depends on its efficiency, which varies from hour to hour depending on the local climate conditions and is measured using the Seasonal Performance Factor (SPF). The 2013/114/EU guideline [46] considers an electric HP to be a renewable system providing the SPF is higher than 2.5 and in addition, manufacturers must estimate the SPF of their devices according to EN14825:2012 [47].

Nevertheless, when operating alone, electric ASHPs present some shortcomings. Firstly, the higher the gap between the outside air and fluid outlet temperatures (air or water), the lower the capacity and efficiency, occurring in the coldest and hottest periods of the year, when air conditioning is most necessary. In addition, if the ASHP is designed to cover the building's entire thermal demand, it cannot fully cover the DHW demand all year round given the DHW high design heating load, creating a

storage volume to level the loads necessary [44]. This disadvantage can be addressed through the integration of a back-up energy source with a water tank, which some authors have described as a “bivalent HP system” [48]. The second heat generator works whenever the ASHP operation is not economically or ecologically reasonable and it supports the ASHP when its capacity cannot cover the energy demand of the building. The second shortcoming has to do with the fact that air is an intermittent RES. Therefore, the pattern defining the performance of an ASHP is not linear and depends at each instant on the outdoor air temperature, supply temperature and heat load. As a result, calculations have to be made on an hourly basis using reliable local climate data and dynamic energy simulation tools. Regarding the third disadvantage, the non-renewable primary energy (nrPE) consumed by an ASHP depends on the electricity share produced from RESs in the PEG mix, which varies every hour depending on weather conditions and is also non-linear, making it particularly difficult to measure the savings accurately. Some authors [49] calculate it on the basis of the primary energy factor (PEF), which is a national specific yearly average of the hourly-variable amount of nrPE contained in each generation system. Others [41] propose a higher resolution method, based on the increasing available information on the power mix of many EU countries, and requiring the establishment of specific hypotheses about the conversion efficiency of the power plants supplying the network. In Spain, as in most EU countries, the shareof RESs in the electricity mix cannot be planned in advance and the PEF is conservatively established by the Government in seven-year periods in order to make it dependent on the generation structure and not on the climatic conditions of each year. According to official records [36], in 2016 renewable and non-renewable shares in the Spanish electricity mix were 40.8% and 59.2% respectively. For 2017, the year used for simulations in this paper, the renewable share decreased to 33.7%. This mismatch is assumed by the authors in the calculation of the nrPE consumed by the case-study building.

An important contribution of this work is related to the fact that while hybrid systems based on ASHPs have usually been considered a strategy for the decarbonization of the heating sector in cold climates, analysis for mild climates is less frequent despite some exceptions [37,38,50–52]. The application of a hybrid system to produce energy for space air-conditioning and DHW throughout the year as part of the retrofit strategy of historic residential buildings in Mediterranean climate has been barely used so far.

2. Case study description.

The case-study building is an 18th-century residential building located in San Gil neighbourhood (overlooking Calle Sagunto), in the north of the conservation area of Seville, Spain. An aerial view of this part of the city is shown in Fig. 1. This conservation area contains 11,029 buildings, 98% of which

are housing, and is catalogued at regional level under the highest protection grade existing in Spain. It occupies almost 6% of the total municipality area, with 9% of its total population, and 62% of its buildings are protected. Within its perimeter, the urban complex of the “Cathedral-Alcázar-Archivo de Indias”, included in the World Heritage List, conditions the urban transformations in a 100-metre radius, or beyond if it affects visual integrity [53]. This conservation area is covered by a Special Protection Plan [54] containing binding policies on urban infrastructures, building conservation, refurbishments and demolition. The listed building stock is classed according to four grades: A and B for monuments; C for buildings of typological interest; and D for buildings which contribute to maintaining urban identity.

Fig. 1. Aerial view of the north area of San Gil neighbourhood, within the conservation area of Seville [54]. The remains of the 11th-century city wall can be seen in the upper right-hand corner. The case-study building, overlooking Calle Sagunto, is highlighted in thick black lines.

Seville is located in the southwest of the Iberian Peninsula, in a Mediterranean climate zone, subtype Csa in the Köppen-Geiger-Pohl system [55]. It has a warm temperate climate with hot dry summers and rainy mild winters and is included in zone B4 of the Spanish climatic zoning, with the highest value in the scale of summer climate severity. Since ASHP performance largely depends on the actual outdoor air temperatures (OAT) of each particular year, historic climate data were compared to those for 2017 (Fig. 2), used for simulations in this research. Both sets of data were obtained from AEMET [56]. The comparison reveals significantly higher daily maximums for 2017 (7 ℃ on average for the twelve months) which increases the ASHP efficiency in heating periods but lowers it during cooling ones. The OATs during June and October of 2017, with average daily temperatures of 28 ºC and 24 ºC respectively, 3 ºC and 4 ºC above the historic data, are especially unusual. The summer of 2017 was particularly hot in Seville. For 40% of summer days, “outdoor temperatures were above 40 ºC, the cut-off point for activating heatwave protocols, and five heatwave periods were recorded, with minimum outdoor temperatures rarely below 20 ºC and maximum temperatures up to 47.4 ºC” [57]. This climate scenario seems to reflect the projections included in the 2017 EEA Report [58] according to which the increase in the global surface temperature is expected to affect the frequency and

intensity of extreme events, such as extreme heat so that “more frequent very hot days and nights, longer warm spells and more intense and frequent heat waves are projected for the whole Mediterranean region”. In view of this, it is realistic to assume that our findings can be extended to other years in the near future.

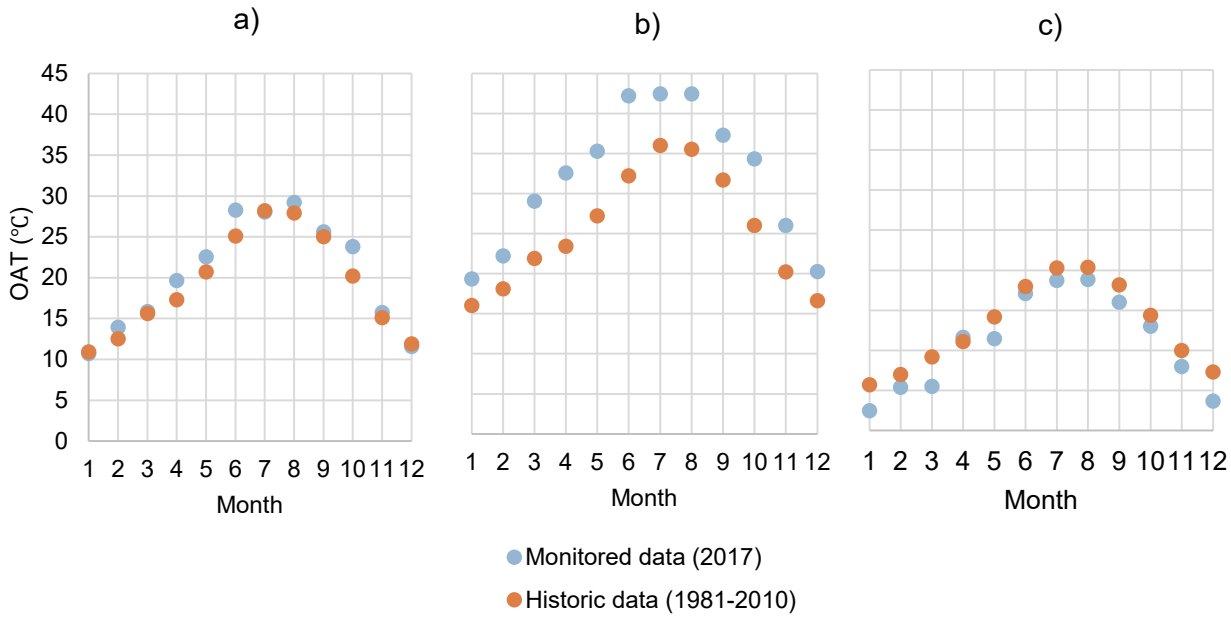

Fig. 2. Scatter plots showing the monthly evolution of OATs in Seville. Blue dots are for 2017 measured OATs and orange dots are for historic data (1981-2010). Average rates are depicted in (a), maximums in (b) and minimums in (c).

The building case-study presented in this paper is typologically classified in the Special Protection Plan of Seville as a “Corral de Vecinos”, a popular multi-family building where the dwellings, with one or two rooms, are distributed around a common patio (or patios) which they overlook from galleries that also provide access. The common patio, carefully landscaped and cared for, provides lighting and ventilation to the individual dwellings and is a space for social interactions (Fig. 3). These buildings were traditionally two-storeys high but most of them have now added a third floor (Figs. 3 and 4). “Corral de Vecinos” buildings account for 12.5 % of the residential buildings within the Sevillian neighbourhood of San Gil [59]. The case-study building is a very well-preserved example of its typology, and unlike others which have been subject to unfortunate major interventions resulting in the loss of much of their character, it offers a good opportunity to investigate the true potential of an ambitious energy retrofit that does not neglect the protection of its values. Its 510 m^2 usable floor surface is divided into three floors, with a net volume of 1,907 m^3 and 13 dwellings with an average usable surface of 39 m^2 (Fig. 5). Refurbishment work carried out in 1992 improved the roof waterproofing, plumbing, water and electricity networks, façade finishes and carpentries but did not

take into consideration energy conservation issues. When existent, the air conditioning is supplied room by room with portable electric oil radiators and/or air-to-air heat pumps, of various ages and states of disrepair. The DHW is produced with electric water heaters (EWHs). The only form of ventilation is natural, through windows, although mechanical vents are found in bathroom and kitchen ceilings (these are poorly maintained and did not work properly for most of the dwellings). The sole source of energy supply is the PEG.

Fig. 3. Street view showing Calle Sagunto and the main entrance to the building (photo on the left) and images of the common inner patio, which provides access to the dwellings (two right-hand-side photos).

Fig. 4. Images of the flat roofs above the first and second floors of the case-study building.

In the municipal catalogue of building protection, the building is listed under level C. Together with D-listed buildings, C-listed buildings account for 96% of the total listed building stock in Seville [54]. Conservation and extension work respecting all alignments is allowed for all buildings. The elements protected are: spatial configuration of patios and of the entrance-stairs-patio grouping; main beam span; roof typology; original façade colour, materials, and ornamental elements, including cornices; size, form and mouldings of façade openings; carpentries and artisanal ironwork. Although this local regulation prevents the external thermal insulation of façades it allows roof insulation and the

replacement of window glazing and frames for new ones with a similar appearance to the original ones. Both these measures constitute the prevalent, and practically only, retrofit variant applied to the vast majority of historic housing in Seville. The regional heritage legislation protecting the historic urban landscape from visual pollution [60] is applicable to the conservation area of Seville. Although it does not explicitly prohibit the installation of RESs or other high-efficiency systems in historic town centres, its implementation is hindered by extensive administrative procedures, so that ambitious decarbonization measures are generally ruled out.

Fig. 5. Floor plans of the case-study building. Dwellings are numbered and communal spaces coloured in light ochre. P: patio, T: terrace, FT: flat roof (also used as a terrace).

3. Materials and methods.

The method consists in simulating two different energy scenarios for the case-study building and carrying out a comparison of results for final and PE consumption. The first case (Base Case, BC) represents the building in its current state, with no RES. The input data needed for the construction, simulation and validation of the model were obtained from an energy audit carried out in one of its dwellings in 2017. The second, built on the BC diagnosis, represents an optimized scenario (Optimal Case, OC) in which the building is comprehensively energy retrofitted, addressing the environmental and health deficiencies identified and taking into account heritage conservation constraints. The package of retrofitting measures simulated in the OC included both passive and active actions, as well as RES integration to cover all thermal energy needs in the dwellings. The BC baseline thermal system consisted of split room air-conditioners, with a COP and EER equal to those found in the monitoring campaign, and an EWH. In the OC a hybrid system was modelled, consisting of an air-to-water reversible heat pump (ASrHP) and an electrically driven water heater (EWH) operating in parallel mode. The auxiliary EWH is a back-up system, supporting the HP when its capacity is not sufficient to cover thermal demand, as described in the Introduction, and ensures that the outlet temperature of 60 ºC is reached in the storage tank to prevent the proliferation of legionella.

Both models were simulated and examined in a full-year dynamic numerical simulation. Their outputs on final and PE consumption were then benchmarked against the mandatory limits imposed for non-listed buildings in the same climate zone. As previously mentioned, listed buildings are exempt from compliance with the national energy code (NEC). However, in this research, the NEC threshold [61], which aims to upgrade the existing residential buildings to NZEB levels, was considered for reference. For thorough renovation of residential buildings in climate zone B, NEC upper levels are set at 80 kWh/m^2 year (for total PE consumption) and 55 kWh/m^2 (for non-renewable PE consumption). The dynamic simulation software used for this research was Design Builder (v.6.1.0.6), which employs the calculation engine Energy Plus 8.9 [62], a tool created by the U.S. Department of Energy [63] and globally recognized by the scientific community.

This method can be summarized as a three-step process: (1) BC construction, simulation and validation; (2) BC assessment and diagnosis; and (3) OC construction, simulation and analysis. The diagram in Fig. 6 depicts the energy models generation process.

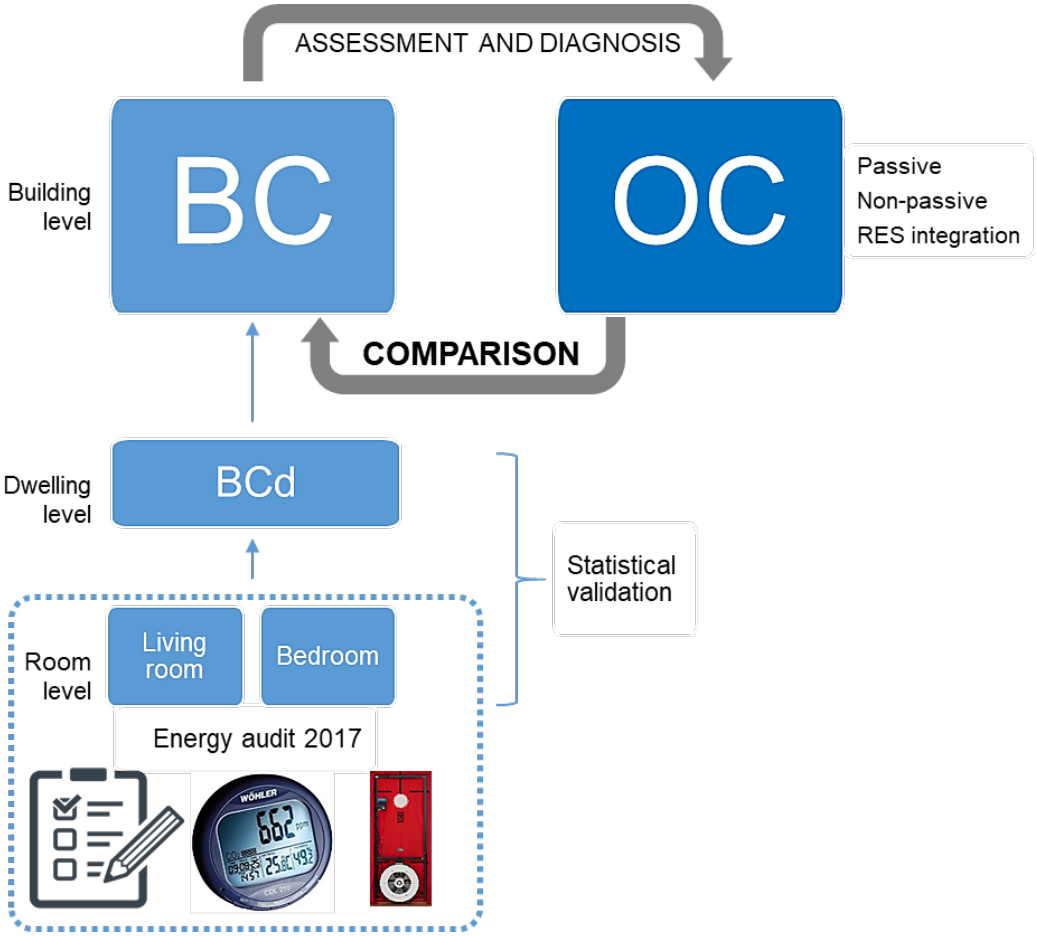

Fig. 6. Diagram summarizing the generation process for the two energy models.

3.1. BC construction, simulation and validation.

The BC model was constructed, firstly scaling up from room level (BCr) to dwelling level (BCd) and secondly, to building level (BC). Three steps were needed to complete this task:

1º A sample dwelling, located on the top floor of the building and containing two main spaces, living room and bedroom, was audited in 2017. The study included a monitoring campaign and in situ inspections, as well as personal interviews with the residents to faithfully characterize the user patterns affecting energy performance. Three physical parameters were monitored in both rooms during summer and winter: indoor CO_2 concentration, indoor air temperature (IAT), and relative humidity. The Blower Door Test was carried out to measure the airtightness of the envelope (n50). Climate hourly data for 2017 were obtained from two AEMET [56] meteorological stations located in Seville. The two BCr models were manually adjusted to ensure precision and their outputs were then statistically validated through the comparison of measured and simulated IAT rates for each room over an eleven-day periods in both winter and summer. Its results on thermal comfort (TC), IAQ and energy performance were published recently [64,65] by the same authors.

2º Using the BCr models as a starting point, a new model of the whole dwelling (BCd) was generated by deleting its internal partitions and adding their equivalent thermal mass. Operational patterns were adopted from the BCr model and correspond to those derived from the audit findings. The IAT rates measured for living room and bedroom in grades centigrade (ºC), obtained through monitoring, were averaged and used to statistically validate the BCd model by comparing them to the simulated IATs. BCd statistical validation was carried out following the M & V Guidelines of the U.S. Department of Energy [66], which employs two indices for the quantification of the error, Mean Bias Error (MBE) (formula 1) and Coefficient of variation of the Root Mean Square Error (CvRMSE) (formulas 2 and 3). An energy model is considered to be validated if MBE hourly values fall within ±10% and CvRMSE falls below 30%. BCd validation results are shown in Section 4.1.

$$\text{MBE (\%)} = \frac{\sum_{i=1}^{N_i}(M_i - S_i)}{\sum_{i=1}^{N_i} M_i} \times 100 \quad (1)$$

$$\text{CvRMSE (\%)} = \frac{RMSE}{\frac{1}{N_i}\sum_{i=1}^{N_i} M_i} \times 100 \quad (2)$$

$$\text{RMSE} = \sqrt{\sum_{i=1}^{N_i} \frac{(M_i - S_i)^2}{N_i}} \quad (3)$$

where: N_i is the number of records used in the validation, S_i is the simulated data at instance, M_i is the measured data at instance n and RMSE is the Root Mean Square Error.

3º On the basis of the adjusted BCd model a third one (BC) was built, including the thirteen dwellings of the building, each considered as a thermal zone. Input data on the current physical state of the envelope were adopted from the previously validated models (BCr, BCd) based on the data gathered in the 2017 audit, including n50 and U-value of walls, windows, roof and floors. In the remaining twelve dwellings the type of technical system for heating, cooling and DHW production and its efficiency (COP and EER) were also assumed to be identical to that existing in the audited dwelling. The existing system of solar shading of openings, consisting of traditional wooden roll-up blinds, was maintained in the BC model. For all the façade openings, window shading schedules were optimized following the conclusions of León et al. [67] for a residential building located in Seville. The authors quantified the reduction in energy demand achieved according to different types of solar protections, including that with horizontal louvres observed in the case-study building. They found that the lowest annual energy demand occurred when the opening-closing program was set to a specific timing in which the blinds were 100% closed from 0-24h from May to September and 100% open from 0-24h from October to April, for all four solar orientations. Internal gains and operational conditions for

occupancy, lighting and use of electric appliances were homogenized to those of the NEC to ensure comparison of results for different dwellings. The same process was followed in relation to HVAC periods of operation, schedules and set-point temperatures. Natural ventilation patterns (rate and timing) were adopted based on the 2017 user-profile investigation and subsequently validated in the BCr and BCd models. A summary of the input data for the BC model is presented in Section 4.2.1.

3.2. BC assessment and diagnosis.

TC was evaluated at both floor and building level, considering the average rates of simulated IATs for independent dwellings. Two indices were used for the floor-level evaluation: (1) percentage of occupied hours of discomfort (OHD) (%) and (2) average deviation from T_{op} (ºC). Results were consistent with the previous analysis at room and dwelling level carried out by the authors [64,65]. Since the dwellings are simulated as being mechanically heated and cooled, following NEC, the criteria for the building-level evaluation were based on the indices of PMV (Predicted Mean Vote) and PPD (Predicted Percentage of Dissatisfied) following EN 16798-1 [68]. The target thermal conditions were set at -0.5 <PMV<+0.5 for PPD<10% (Category II). The design values for clothing, metabolic rates, and air speed for winter, mid-season and summer are shown in Table 1.

Table 1
Design values for thermal comfort evaluation

	Clothing (clo)	Metabolic rate (W/per)	Air speed
Winter (1/1-31/3, 1/10-31/12)	1	180	0.1
Mid-season (1/4-31/5)	0.8	180	0.15
Summer (1/6-30/9)	0.5	180	0.15

Energy performance was studied at building level by analysing BC simulation outputs on thermal loads in kWh/m^2 over the entire year, along with its monthly evolution. The contribution of both the building-driven and user-driven factors to the overall balance was examined separately. PE consumption was calculated using the official 2016 PEF of the Spanish electricity mix [69]. When energy supply comes exclusively from the PEG, these coefficients are:

$$2.007 = \frac{\text{Non} - \text{renewable primary energy (kWh)}}{\text{FE from public electricity grid (kWh)}}$$

$$0.396 = \frac{\text{Renewable primary energy (kWh)}}{\text{FE from public electricity grid (kWh)}}$$

Finally, a complete diagnosis of the BC model was reached and a package of improvement measures, both passive and active, was established. Passive measures consisted in the reduction of the U-value

of non-protected exterior walls, glazing, and roof and the increase in the air tightness of the envelope to regulatory limits. In addition to a mechanical ventilation system (MVS) to guarantee IAQ conditions under the higher air tightness, active measures included the integration of RESs for the production of all thermal energy.

3.3. OC construction, simulation and analysis.

The OC model was constructed by adding the measures mentioned above to the reference model, BC. Therefore, OC represents a building in which the envelope thermal characteristics are improved to their maximum capacity considering the limitations of heritage regulations. In addition, air conditioning schedules are adjusted to the actual comfort demand, IAQ is ensured by the natural and MVS operation and PE consumption is as close as possible to the NEC upper limits, thanks to RES integration using a hybrid energy system.

The U-value of patio-block walls and roof was reduced to mandatory limits by modelling thermal insulation, as permitted by heritage conservation regulation. Stone-wool insulation was adopted for both cases: λ=0.031 W/mK, δ=40 kg/m^3, 4-cm thick for the patio-block walls, added externally, and λ=0.035 W/mK, δ=150 kg/m^3, 6-cm thick for the roof. n50 for the OC scenario was calculated following the method set in NEC. This uses a formula which employs standard reference values, under 100 Pa air overpressure, for air flow through opaque surfaces of refurbished or existing building envelopes (C_o) (16 m^3/hm^2 for new or refurbished and 29 m^3/hm^2 for existing buildings) and for the air tightness of openings (C_w) following the categorization of EN 12207-2016 [70]. For the OC state the following reference values were adopted: C_o= 16 m^3/hm^2, C_w = 27 m^3/hm^2 (Class 2, minimum required by NEC). The n50 rate obtained was 3.71, as shown in Table 6. The modelled MVS was dual flow with heat recovery (enthalpy 85%). It extracted air from wet rooms, recovering energy from them through a heat exchanger (efficiency 92%) and preheated or precooled the incoming air. It was sized following the national regulation [71], which set a continuous rate for air exchange of 86.4 m^3/h per dwelling (0.7 ach^{-1}) to ensure that the annual average CO_2 concentration in each room is below 900 ppm and that the annual cumulative CO_2 exceeding 1600 ppm is less than 500,000 ppm·h. The system has three elements connected to the PEG, the electricity consumption of which was calculated at 2.79 W/m^2 based on the set flow rate of each dwelling.

RES integration aimed at lowering the fossil-fuel energy consumption was carried out through a hybrid system combining two energy conversion devices: a renewables-based one, a highly efficient reversible air-to-water heat pump (ASrHP), and a non-renewable one, a supplementary EWH, as

mentioned above. A schema is shown in Fig. 7. The large air heating/cooling design loads are met at high-speed variable-speed compressor operation while the smaller water heating loads are met at lower speeds [45]. During periods of heating demand, the HP heats the water in a closed circuit connected to the terminal units: fan coils (outlet air temperature of 35 ºC) and an EWH (outlet temperature of 55 ºC). It runs at maximum capacity to heat the water stored in the tank whose temperature must be maintained at 60 ºC. When DHW is required, a three-way valve allows the water flow to be diverted through the tank in the indoor unit. In summer, the HP produces cold water at 7 ºC which is circulated to the fan coils to cool the air.

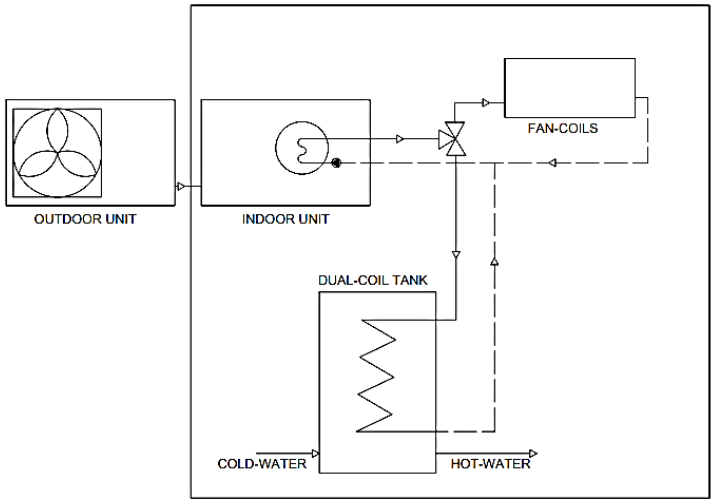

Fig. 7. Hybrid system scheme.

ASrHP was sized to cover the heating and cooling loads calculated for each building floor according to the nominal capacities of the manufacturer. The DHW demand was calculated following the NEC [71] which set a reference demand of 28 l/person·day (0.012 m^3/h·person) and a minimum instantaneous flow of 2.9 m^3/h per dwelling for a water temperature of 60 ºC. The modelling input parameters and their values, as well as the nominal capacities of the HP, are summarized in Table 2.

The system described was modelled and examined in a full-year dynamic numerical simulation. Dynamic numerical simulations of hybrid systems had previously been undertaken [42,45,48,50] using different tools. The Energy Plus engine was used to simulate a hybrid system similar to that designed by Shen et al. [72], who in 2017 calculated annual energy savings averaging 56% for a commercial building in ten different climate locations in the USA. It was also employed by Torregrosa et al. [52] in 2018, who studied a residential building under different Spanish climates, comparing the results to a conventional HVAC system. In this research, the system was modelled in Energy Plus 8.9 via EMS language, as in [72] and [52], adjusted to the data provided by the manufacturer on energy rating, capacity and electricity consumption of the devices, at different outdoor air and chilled water

supply temperatures, as well as at different partial load ratios. In the periods of heating/cooling demand Energy Plus calculates the energy rate to cover air conditioning and DHW production, as well as the electricity consumed by the EWH to complement the DHW needs and by the auxiliary systems (fan and pumps), all on an hourly basis. During inter-seasonal periods, where the OATs show major variations within the same day and from one week to another, ASrHP capacity varied accordingly and the hot water it produced presented intermittent patterns. For each floor, the following hourly output data, in watts, was uploaded for analysis: (1) Total heating rate, (2) Total evaporator cooling rate, (3) Water use equipment heating rate, (4) Water heating electric power and (5) Auxiliary systems electric power: fans, pumps, VS compressor. These simulation outputs were analysed for the whole year and for the three floors of the building, providing an estimation of the hourly energy rate and electricity consumption of the ASrHP and EWH separately to study its evolution across the different seasons.

Table 2
Input parameters and values of the Integrated HP.

ASrHP outdoor unit	
Air heating	
Flow type	Variable
Schedule	On 24/7
Water outlet nominal temperature	55 ℃
Minimum temperature inlet air	-10 ℃
Nominal capacity	6800 W
COP	3.76
Air cooling	
Flow type	Variable
Schedule	On 24/7
Water outlet nominal temperature	7 ℃
Reference inlet air temperature	29.4 ℃
Nominal capacity	6100 W
COP	3.67
ASrHP indoor unit (fan coils)	
Air heating	
Supply air temperature	35 ℃
Heating sizing factor	1.25
Air cooling	
Supply air temperature	14 ℃
Cooling sizing factor	1.15
EHW	
Water temperature (inlet)	Monthly evolution according to Annex G of NEC [73]. For Seville, average of 16 ℃.
Water temperature (outlet)	60 ℃
EWH efficiency	0.9
Minimum instant flow	
Floors 0 and 1	0.0042 m^3/s
Floor 2	0.0025 m^3/s
Schedule	6-24 h

Based on the simulation outputs, the ASrHP monthly average efficiency was calculated and represented in a graph (Section 4.2.2), to establish in which part of the year the HP was more efficient

and the savings in fossil-fuel energy were higher. SPF was also calculated, confirming that it far exceeds the minimum value set by the EU Commission [46] to be considered as a renewable system. Finally, the total electricity consumption breakdown, grouped into final (FE) and primary (PE) and thermal and non-thermal uses, was calculated for both the BC and OC scenarios and compared in terms of total, renewable and non-renewable PE consumption, following the diagram of Fig. 8. After this, the rates obtained were benchmarked against the regulatory limits.

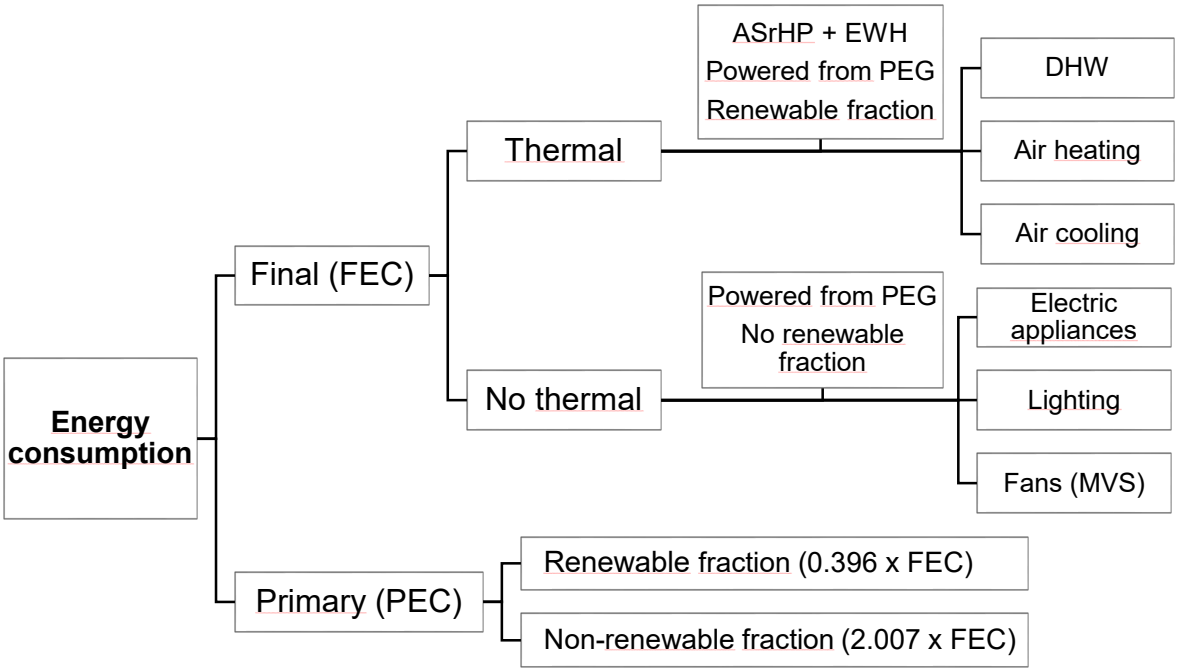

Fig. 8. Diagram showing the schema for calculating the electricity consumed in the BC and OC models.

4. Results and discussion.

4.1. BC model.

BCd (original status, dwelling level) was constructed, simulated and statistically validated following the procedure described in Section 3. Validation results, revealing a high degree of adjustment, are shown in Table 3. On the basis of this adjusted BCd model, BC was constructed, containing the thirteen dwellings, as described in Section 3. BC input data are presented in Section 4.2.1.

Table 3
Statistical validation of BCd model

	MBE	CvRMSE
Winter	-0.94%	4.24%
Summer	-0.25%	2.70%
Limit [74]	< 10%	< 30%

4.1.1. BC Thermal comfort evaluation.

Annual hourly evolution of simulated IATs (℃) for each floor is shown in Fig. 9, obtained by averaging hourly rates for dwellings. Based on this, two comfort indexes were used to evaluate TC conditions at floor level. Results are shown in Table 4.

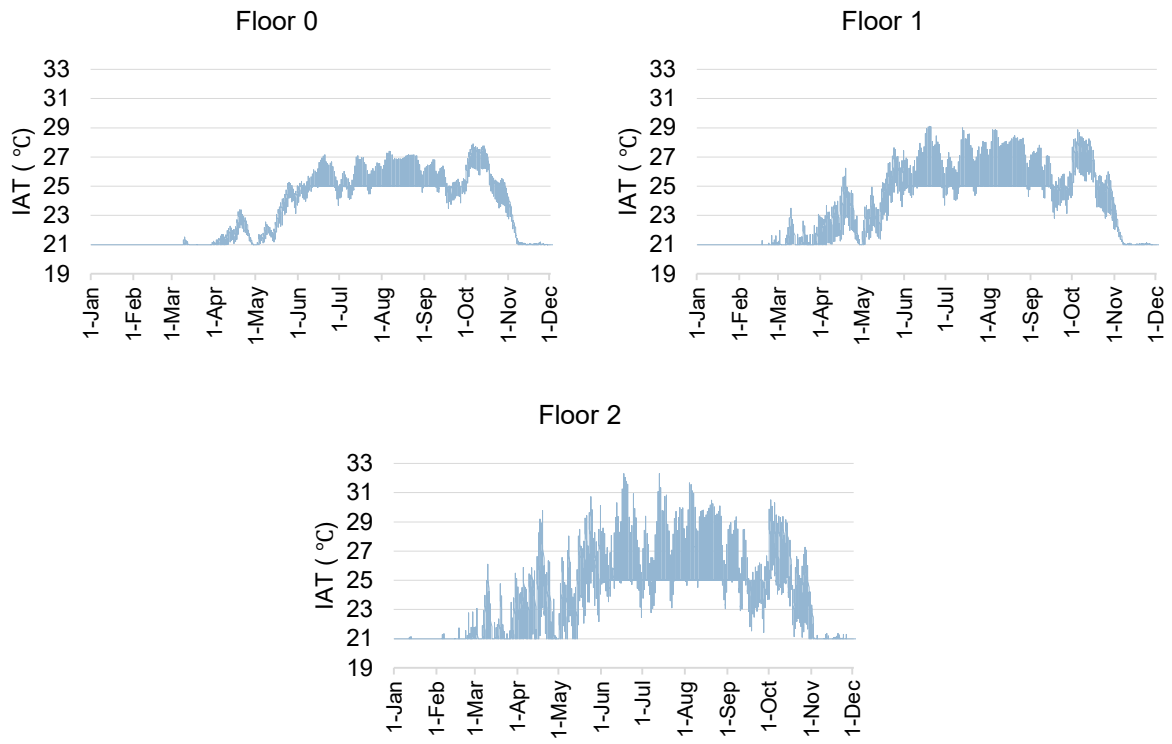

Fig. 9. Annual hourly evolution of IATs (℃) for the three floors of the building in the BC model. On the horizontal axis, labels represent the first day of each month.

Table 4
Thermal comfort analysis by floor during 2017 in the BC model.

	Annual percentage of OHD			Average deviation from T_{op} (℃)	
	Total	Cool	Warm	<21	>25
Floor 0	17%	0%	17%	0	1.1
Floor 1	20%	0%	20%	0	1.3
Floor 2	20%	0%	20%	0	1.9

At building level, TC evaluation was based on the PMV following EN 16798-1 [68]. The annual hourly evolution of PMV, conforming to the set conditions described in Section 3, is depicted in Fig. 10. In view of these results, the dwellings can be considered thermally comfortable during winter due to the continuous operation profile set in NEC. An exception occurs in October, when IAT hourly rates exceeded 26 ℃ for 48% of the occupied hours, as thermal discomfort is associated with excessively high temperatures (Table 4) rather than low ones, despite the intense use of the cooling system set

in the NEC profile (16 hours per day). Two excessively hot periods were identified: (1) October, between 12-24h and (2) from May 15th to September 15th between 11-14h (Fig. 10). The first of these periods is due to a mismatch between the NEC profiles and the climatic reality of Seville, thus according to the NEC, October is considered a heating-demand month, despite the fact that average and maximum daily OATs for 2017 in Seville were about 24 ℃ and 31 ℃ respectively, making cooling more necessary (see Fig. 2). This mismatch also causes the thermal discomfort registered in the second half of May, for which NEC profiles do not set a cooling operation despite reaching maximums of 35 ℃, as also shown in Fig. 10b. Lastly, summer discomfort is caused by the absence of cooling scheduling in the 7-15h time slot set in the NEC standard profile, even though occupancy is in fact considered.

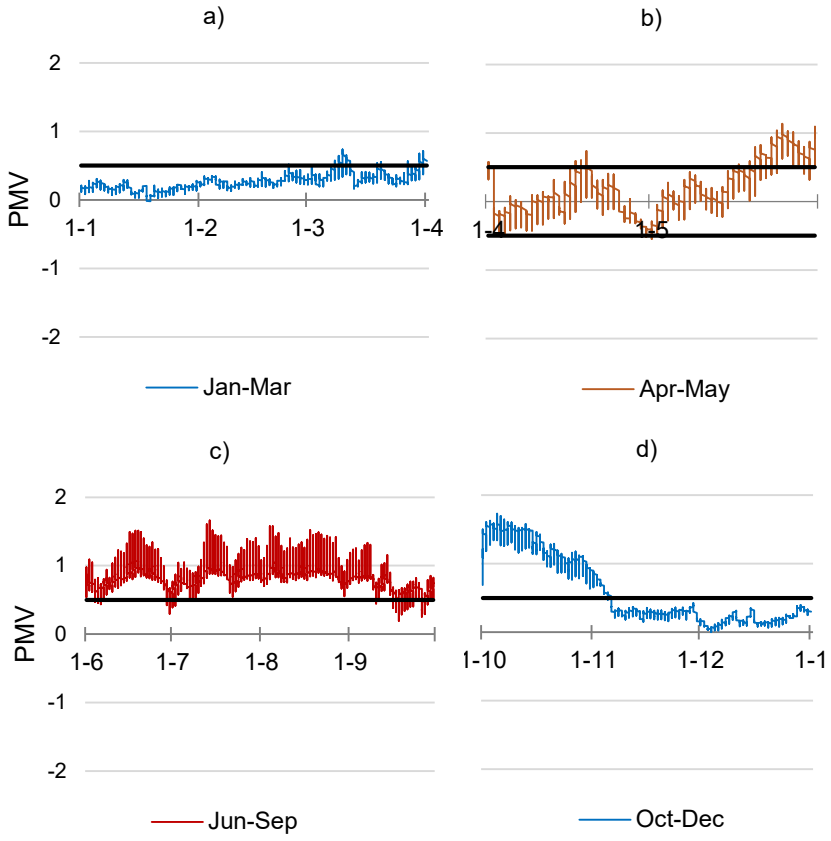

Fig. 10. PMV hourly evolution for winter (a, d), mid-season (b) and summer (c). The limit recommended by EN 7730 for Category II is highlighted in continuous black lines.

4.1.2. BC energy assessment.

Simulation outputs on total thermal loads over the whole year in kWh/m^2 were analysed at building level (Fig. 11a). Building-driven and user-driven loads were studied annually (Fig. 11b) and monthly (Fig. 12) to ascertain the positive or negative contribution of each element to the overall balance.

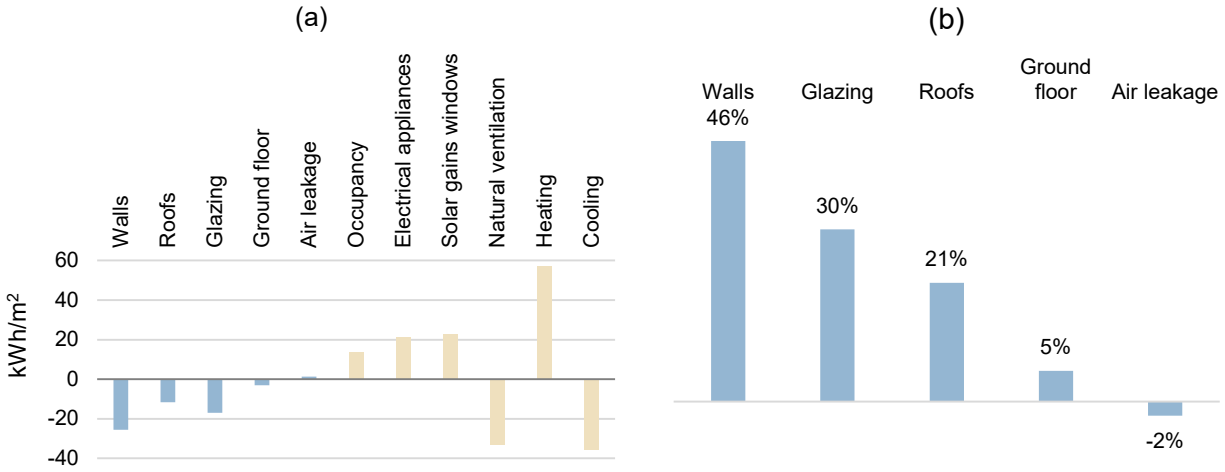

Fig. 11. On the left (a), thermal loads of the building for year 2017. On the right (b) the percentage of individual elements' contribution to the overall building-driven heat losses during that year.

These results, consistent with those previously obtained by the authors [64,65] from an energy audit on a sample dwelling reveal that, in the case of building-driven factors, all constructive elements but the ground floor have a detrimental impact both in summer and winter. The poor air tightness of the envelope also causes significant heat losses in winter and gains in summer. When considering the annual balance, walls, glazing and roof are responsible for a large part of the unfavourable effects. As regards user-driven factors, the simulated natural ventilation profile (1.5 ac/h continuously during summer nights and 1 hour per day in early morning for the rest of the year) has a positive effect on the thermal balance of summer and a moderate negative effect on that of winter and mid seasons.

In the BC scenario the building consumed net electricity of 36,672 kWh/year (64 kWh/m^2 year), which is equivalent to a total PE consumption of 150 kWh/m^2·year and to a non-renewable PE consumption of 129 kWh/m^2·year. Both are twice the mandatory limits for non-listed residential building retrofitting in climate zone B4.

4.1.3. BC diagnosis.

When heating and cooling operate according to the NEC standard schedules, significant thermal discomfort is observed from the second half of May to October, while PE consumption is double the maximum permissible value. The unsuitability of heating/cooling schedules and time periods merely requires a simple adjustment, while reduction of PE consumption needs of (1) energy demand decrease and (2) replacement of the inefficient existing mechanical thermal systems, which are intensive electricity consumers are required for the more efficient integration of RES on site.

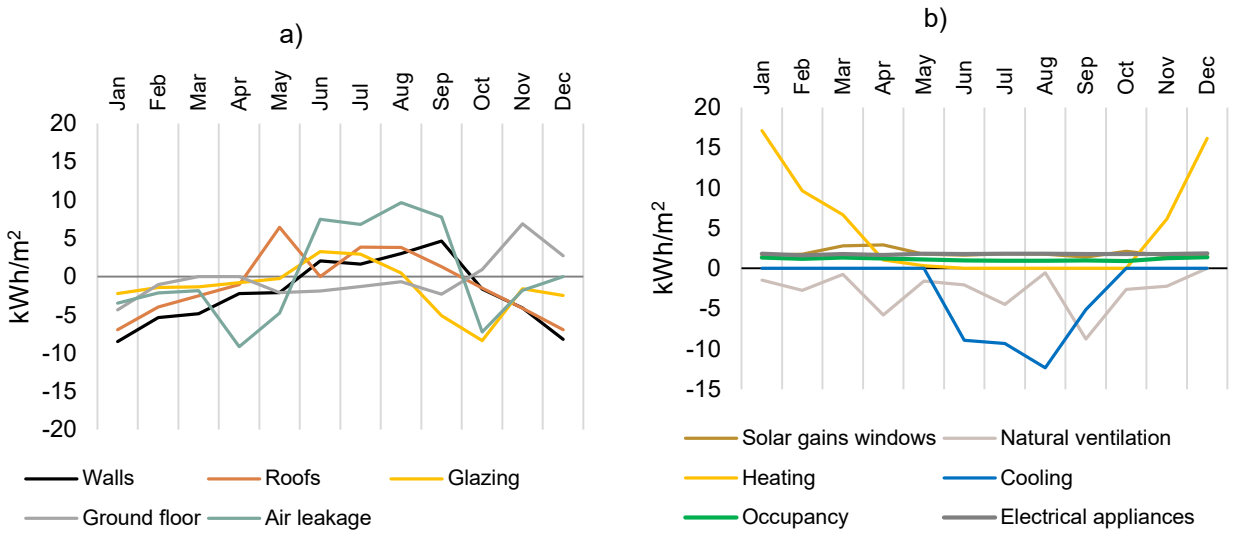

Fig. 12. Monthly evolution of building-driven (a) and user-driven (b) thermal loads calculated at building level for the year 2017.

To achieve this decreased energy demand, unfavourable heat gains and losses through walls, glazing and roof should be avoided by decreasing their U-value and increasing n50. The heritage protection rules to which the case-study building is subject prevent the external insulation of façade walls. Internal insulation is not usually a practical option as dwellings are inhabited, and this would require specific assessment of moisture related risks [75]. Only the non-protected patio-block walls can be externally insulated, although a poor result is to be expected as their surface only accounts for 23 % of the total wall area of the building. Nevertheless, there is ample room for improvement for the U-value of roof, glazing and frames, since these enhancements are permitted by local regulations for C- and D-listed buildings, as previously mentioned. Regarding n50, window frames should be replaced by others with lower air permeability, in compliance with NEC, although the effect could be detrimental. Indeed, as other authors [31], [32] have previously pointed out, in buildings located in the same climate zone with only natural sources of ventilation, the increase in n50 derived from the window upgrades has a unfavourable effect on the CO_2 concentration in residential spaces, especially during winter [65]. Therefore, this measure should be accompanied by an efficient constant flow of

MVS to compensate for the loss of outside air intake. In Spain, this system is mandatory for extensive renovations of non-listed buildings to guarantee the IAQ.

In conclusion, the improvement measures modelled in OC can be summarized as follows: M1. The cooling period is extended from May to October while the heating one is reduced to January-April and November-December. The cooling schedule is broadened to the 11-24h time slot in summer; M2. Thermal insulation is added to patio-block walls and roof to decrease U-value to regulatory limits (U_{wall} < 0.56 W/m^{2}K, U_{roof} < 0.44 Wm^2/K); M3. New double-glazing is also added (with solar control in openings facing south and west). In combination with the new airtight frames (Class 2 of Q_{100lim}= 27 m^3/hm^2, measure M4) the U-value of windows is cut down to the regulatory limit (U_{window} <2.3 W/m^{2}K); M4. Reduction of n50 to regulatory limits; M5. A constant-flow MVS is implemented following the national regulation [71] for the refurbishment of non-listed buildings and M5. An integrated HP is also implemented. Technical features and details of all these measures are described in Section 3.3

4.2. OC model.

4.2.1. Input data.

U-values of the constructive elements in the BC and OC models are compared in Table 5. The main input parameters considered for simulation and their values for both models are compared in Tables 6 and 7.

Table 5
U-value in W/m^{2}K of the constructive elements of the envelope in BC and OC energy models

	BC	**OC**
Protected walls (ground and first floors)	0.75	0.75
Protected walls (second floor)	2.26	2.26
Walls (in block patios, no protected)	2.26	0.53 (*)
Roof	3.10	0.4 (**)
Openings (façade)		
Joinery	1.90	1.49
Glazing	5.78	2.51
Window	6.96	2.31
Openings (patio)		
Joinery	5.88	2.00
Glazing	5.78	1.76
Window	5.80	1.83
Ground floor	1.90	1.90

(*) Added MW Stone wool insulation (λ=0,031 W/mK, δ=40 kg/m3, 4 cm thick) in the outermost layer.
(**) Added Stone wool insulation (λ=0,035 W/mK, δ=150 kg/m3, 6 cm thick)

Table 6
Simulation inputs for the BC and OC energy models.

Model	**BC model**	**OC model**
Activity		
Density	0.03 per/m^2	
Metabolic factor	0.9	
Occupancy schedule	Following NEC (see Supplementary material)	
HVAC		
Heating		
Type	Electric heat pump	ASrHP + EWH
Efficiency (COP)	COP = 2.50	COP = 3.76
Set-point temperature	21 ℃/ 17 ℃	21 ℃/ 17 ℃
Period of use	Jan-May, Oct-Dec	Jan-May, Nov-Dec
Schedule	Following NEC (Table 7)	See Table 7
Cooling		
Type	Electric heat pump	ASrHP + EWH
Efficiency (EER)	EER = 2.60	EER= 3.67
Set-point temperature	25 ℃/ 27 ℃	25 ℃/ 27 ℃
Period of use	Jun-Sep	Apr-Oct
Schedule	Following NEC (Table 7)	See Table 7
Water heating		
Type	EWH	ASrHP + EWH
Set-point temperature	60 ℃	60 ℃
Annual average inlet water temperature	16 ℃	16 ℃
Demand daily schedule	6-24h	6-24h
Daily demand (building level)	1.4 l/m^2 day	1.4 l/m^2 day
Maximum flow rate	0.0042 m^3/s	0.0042 m^3/s
Efficiency	0.9	0.9
Ventilation		
Natural	Opening windows	Opening windows
Flow rate	1.5 ac/h	1.5 ac/h
Period of operation	Throughout the year	Jun-Sep
Schedule	Jan-May, Sep-Dec (7-8h), Jun-Sep (0-8h)	0-7h
Mechanical		
Flow rate per dwelling (constant)		0.7 ach^{-1} per dwelling
Period of operation		Throughout the year
Schedule		0-24h
Heat recovery (enthalpy)	No	On. Enthalpy. Efficiency 85%
Fan total efficiency		92%
Auxiliary energy		2.79 W/m^2
Humidity control		No
Lighting and electric appliances		
Power	2 + 2 W/m^2	
Period of operation	Annual	
Schedule	Following NEC (see Supplementary material)	
Window shading		
System	Exterior. Slatted blinds of pine wood. Roll-up operation.	
Operation	May-Sep always ON, Oct-Apr always OFF	
Air leakage rate at 50 Pa: n_{50} (h^{-1})	7.71 (measured)	3.71 (calculated following NEC)

Table 7
Air conditioning setting in BC and OC models.

Schedule		Jan	Feb	Mar	Apr	May	Jun	Jul	Aug	Sep	Oct	Nov	Dec
Heating	BC	0-24h					-	-	-	-		*0-24h*	
	OC	0-24h				-	-	-	-	-	-	*0-24h*	
Cooling	BC	-	-	-	-	-	0-7h, 15-24h				-	-	-
	OC	-	-	-	-	*0-24h*	0-7h, 11-24h				*0-24h*	-	-
Set point temperatures													
Heating	0-7h: 17℃, 7-23h: 21 ℃, 23-24h: 17 ℃												
Cooling	0-7h: 27℃, 7-23h: 25 ℃, 23-24h: 27 ℃												

4.2.2. Hybrid system performance.

The integrated HP system was modelled following the method described in Section 3. Independent equipment (ASrHP +EWH) was considered for each floor. Three sample days were selected for the daily analysis: winter and summer sample days were those of maximum thermal demand: 5.1 kWh for heating on Floor 0 at 10h on January 22nd and 5.90 kWh for cooling on Floor 1 at 12h on August 8th. A typical spring day (April 18th), where cooling demand is much lower, was also selected. Fig. 13 depicts the hourly evolution of energy demand for air conditioning and water heating and the corresponding ASrHP energy production throughout these typical days. In winter, the air heating is scheduled throughout the day and the energy supplied by the ASrHP largely meets the demand for air conditioning and DHW (Fig. 13a). From June to September, air cooling is programmed in the 11-24h time slot, making it necessary for the EWH to operate from 6h to 11h to meet DHW demand (Fig. 13b). In spring, air cooling demand falls to one third of that of summer. DHW demand produced early in the morning is not covered by the ASrHP but by the EWH. Air cooling needs are fully covered by the heat pump from 11h onwards (Fig. 13c).

Monthly analysis was carried out at building level by adding the hourly rates of the energy consumed and produced by the three simulated systems.The electricity consumed compared to the amount of energy produced in each month is shown in Fig. 14. ASrHP monthly average efficiency is depicted in Fig. 15, showing that these operate very efficiently, especially in the coldest months.

The performance of each HP is depicted in Fig. 16: by month (Fig. 16a) and for the entire year (Fig. 16b). The SPF calculated for the three systems is 4.71, well above the minimum (SPF>2.5) accepted by the EU commission for a HP to be considered as a renewable energy technology. The lowest efficiency is recorded in May and September and the highest for January, February, March, November and December, for both floor and building levels. From June to August efficiency value at building level is around 3. The two most unfavourable scenarios were found in September, Floor 0 and in May, Floor 2, when efficiency dropped to 1.74 and 2.40 respectively.

4.2.3. Domestic hot water production.

The HP produces DHW depending on (1) the air conditioning schedule (if the heating/cooling is not working, DHW demand is covered by the EWH) and (2) the hourly energy demand for air-conditioning and water heating (if the latter is lower than the former, then the water is heated by the auxiliary system). Production of DHW was analysed for the whole year on an hourly basis, separating the hours in which the water was heated by the HP from those when it was heated by the electric back-up

system. The result shows that for 63% of the hours of the year analysed, DHW is produced by the HP and thus by renewable energy. The relation between heating/cooling demand and DHW production for each month is depicted in Fig. 17.

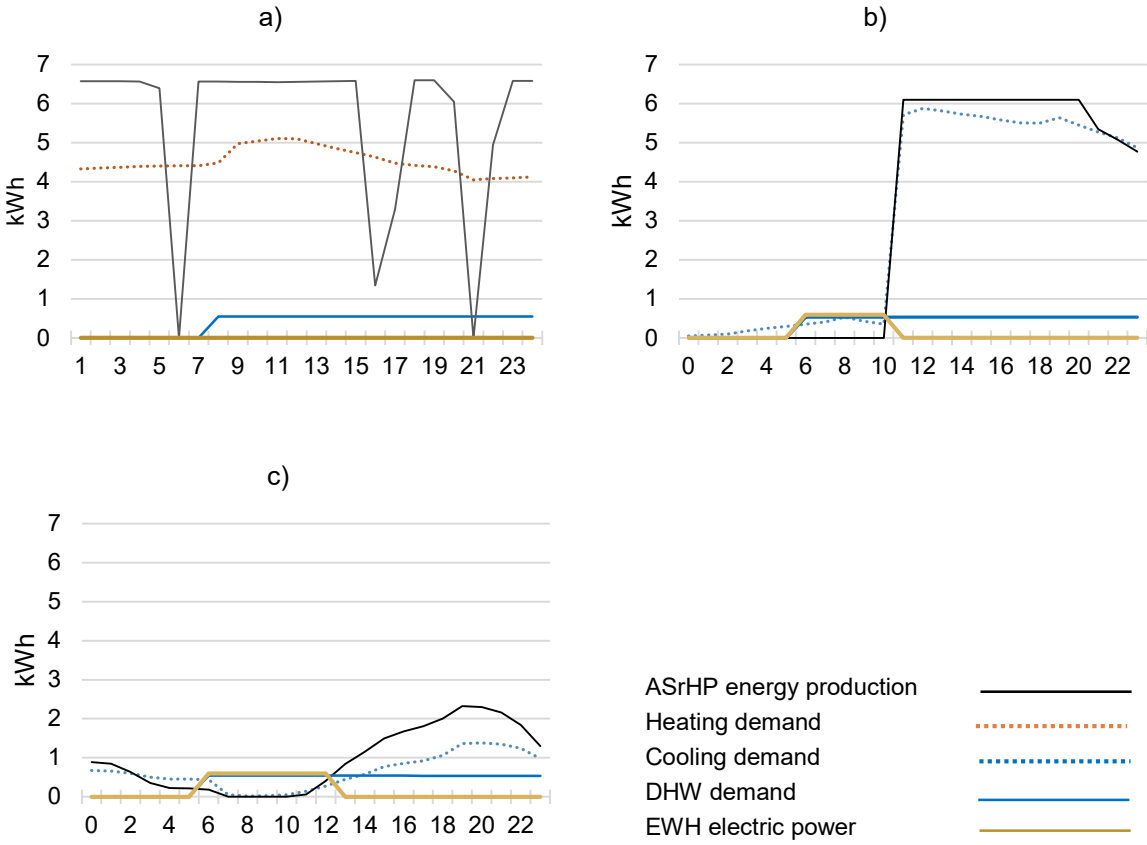

Fig. 13. Winter sample day on Floor 0 (a), summer sample day on Floor 1 (b) and inter-season sample day on Floor 1 (c).

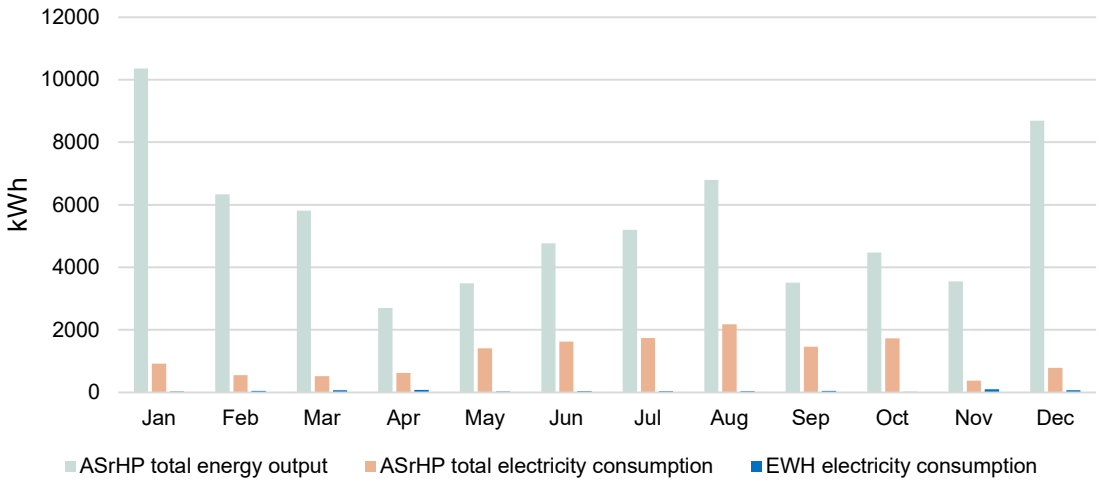

Fig. 14. Monthly evolution of the energy produced and the electricity consumed by the ASrHP in the case-study building, compared to the electricity consumed by the EWH.

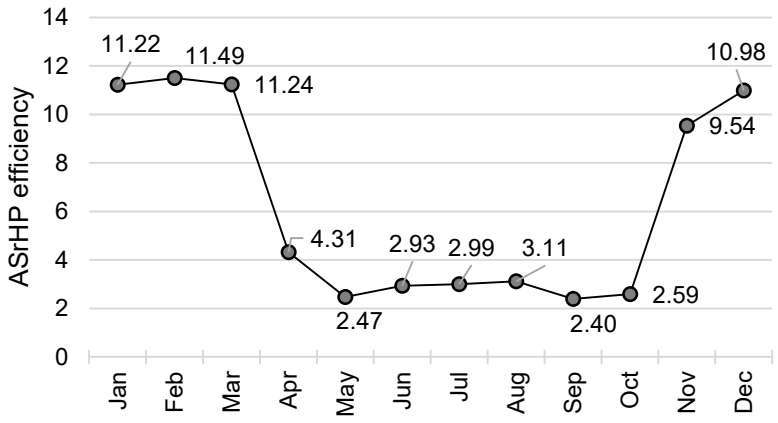

Fig. 15. Monthly average efficiency of the three ASrHPs considered at building level.

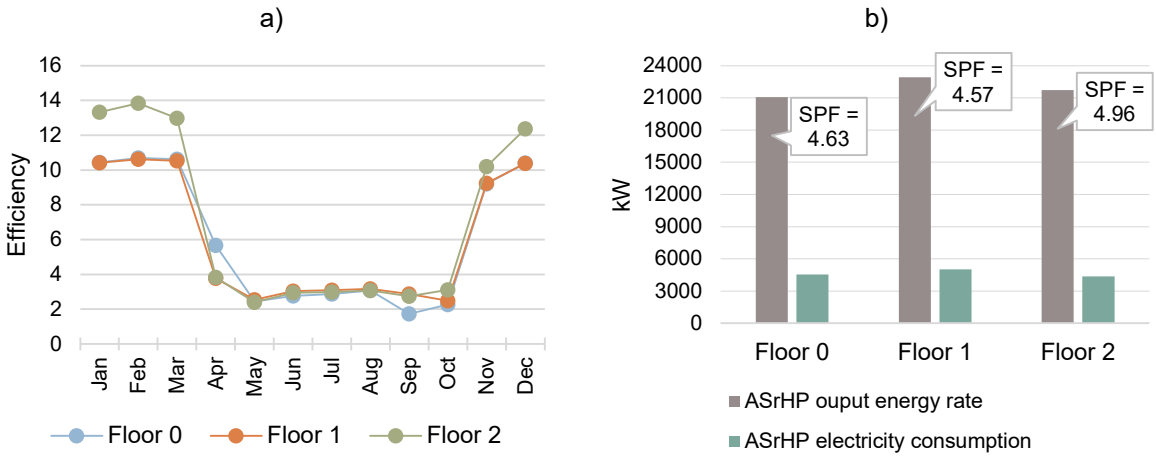

Fig. 16. Monthly efficiency (a) and SPF (b) of the individual ASrHPs considered at floor level.

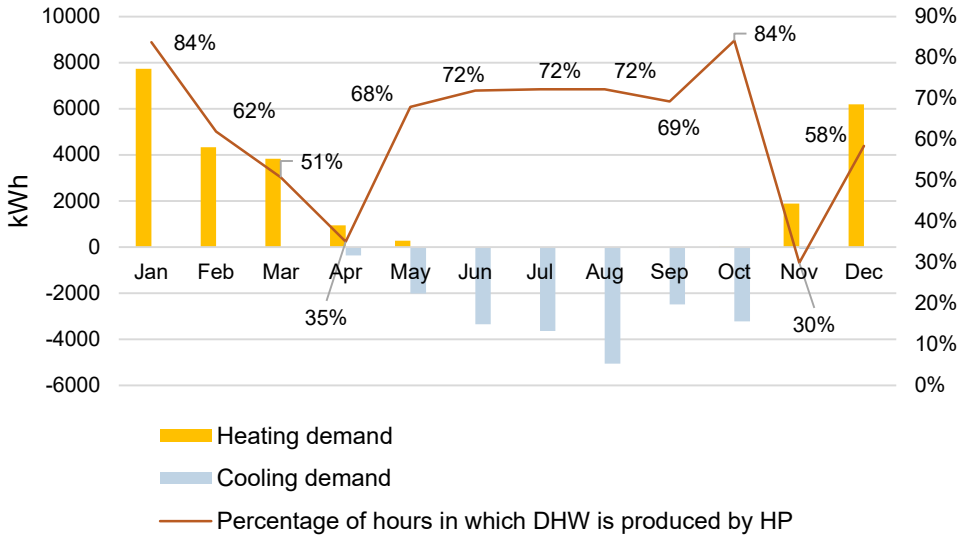

Fig. 17. Percentage of hours of renewable production of DHW related to the energy demand for heating and cooling by month in the OC model.

4.2.4. Final thermal energy consumption.

The FE consumed annually by the thermal services of the building in the OC scenario was calculated according to the hourly simulation outputs. For each sub-system and energy source, the results are presented in Table 8. The main outcomes are: (1) under the OC simulation conditions, 70% of the thermal FE consumed by the building comes from the integrated HP and the remaining 30% is supplied by the PEG; (2) a considerable proportion of the total thermal FE (26%) is consumed by auxiliary systems of the HP; (3) FE consumed for cooling is much higher than that for heating; and (4) the FE consumed by the EHW is very low, since most of the hours DHW is produced by the HP, as described in the previous section.

Table 8
Breakdown of annual final electricity consumption for thermal uses in the OC model (kWh)

Energy source	System	FE consumed	Percentage of total
Air	ASrHP (air and water heating)	2,306	16%
	ASrHP (cooling and water heating)	7,818	54%
	ASrHP total	10,124	**70%**
PEG	EWH	615	4%
	Auxiliary systems	3,809	26%
	PEG total	4,424	**30%**
	Total FE	14,548	

4.3. Comparison of the BC and OC results.

This section presents a comparison of the BC and OC simulation results for energy demand, production and consumption. A summary of the outputs is shown in Table 9 and Fig. 18.

Table 9
Summary of annual energy demand, generation and consumption for the case-study building in the BC and OC scenarios (kWh)

		Energy demand						Energy production	FE consumption	PE consumption
		Thermal			Non-thermal		Total	Total	Total	Total
		DHW	Air heating	Air cooling	Electric appliances + lighting	MVS Fans				
BC		1,780	32,678	20,430	12,260	0	67,148	0	36,672	88,123
	Subtotal		54,888		12,260					
OC		1,780	25,245	20,240	12,260	1,235	60,760	65,685	28,410	51,432
	Subtotal		47,265		13,495					

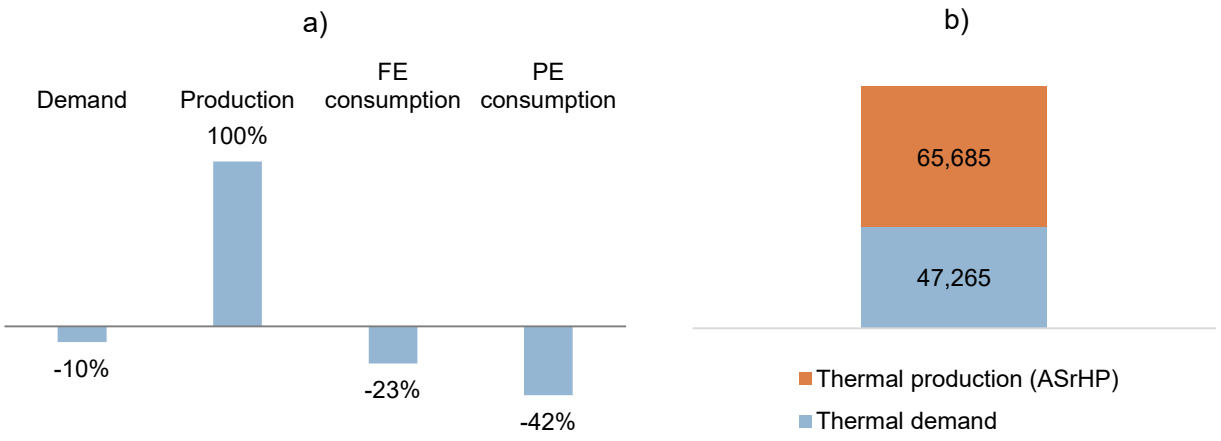

Fig. 18. Percentage deviation in energy demand, production and consumption of OC with respect to the BC scenario (a), and comparison between the thermal demand and the thermal energy produced by the ASrHP modelled in OC (b).

According to these results, the envelope enhancement included in the retrofit plan successfully reduced the overall energy demand by 10%, mainly due to heating, whose demand falls by 23%. In contrast, cooling demand was down by only 0.9%, although this is not an unfavourable result considering that the refrigeration period and timing was extended in the OC scenario with respect to BC to improve the thermal comfort conditions of dwellings. The decrease in energy demand for air conditioning should be highlighted as it indicates that the joint effect of the improvement measures simulated in OC is beneficial in terms of demand. Indeed, some of these measures, such as reduction of n50 and U-value of some elements of the envelope, directly lead to a thermal load reduction in the dwellings. However, when combined with the constant-flow MVS, this beneficial effect may be counteracted, since its continuous air-intake adds an extra thermal load to the spaces. The efficient heat recovery system included in the MVS model can explain this good global performance. Similar results were obtained by Figuereido et al. [76] for a residential building in Aveiro, Portugal, when applying a hybrid MVS with heat recovery and bypass mode for summer; the latter was able to increase the outdoor air flow rate above the initial rate when outdoor air temperatures are lower than indoor ones.

Regarding energy production, the AsrHP modelled in the OC scenario produces 39% more thermal energy than is needed to supply the global thermal demand (Fig. 18b). However, due to the efficiency of this system and its good performance at partial loads, total FE consumption is reduced by 23%, as shown in Fig. 19a, where the FE consumed by thermal and non-thermal uses are represented separately. In Fig. 19b the FE breakdown of thermal services is displayed. Two small increases can be identified, the first due to the MVS fan operation (10%) and the second due to the more extended use of the refrigeration system (7%). Both are counteracted by significant reductions in the FE consumed by air heating (-73%) and DHW (-30%).

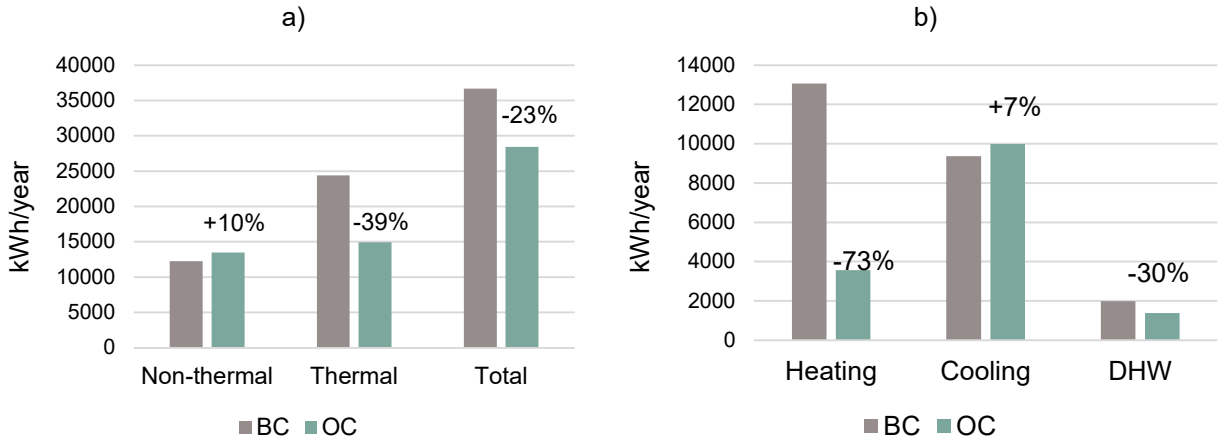

Fig. 19. Annual FE consumed by the building in the BC and OC scenarios. On the left (a) thermal and non-thermal uses are grouped and the total sum is given; on the right (b) the breakdown of thermal uses is shown.

Regarding PE consumption, renewable and non-renewable shares were calculated using the official PEFs approved by the Spanish Ministry [69], as described in Section 3. These were directly applied to all end uses in the BC model, where there was no onsite RES. For the OC model the annually consumed PE was calculated distinguishing between energy sources that feed the thermal systems (see Table 8). The comparison is depicted in Fig. 20.

According to these results, the role of integrated HPs in energy saving is remarkable, since they managed to reduce the FE consumed by the thermal services of the building by 39% (Fig. 19a) and were also responsible for annual savings of 42% (Fig. 20b) in PE consumption of the OC scenario with respect to the traditional solution of the BC model, where air conditioning and water heating are produced separately with low-efficiency devices.

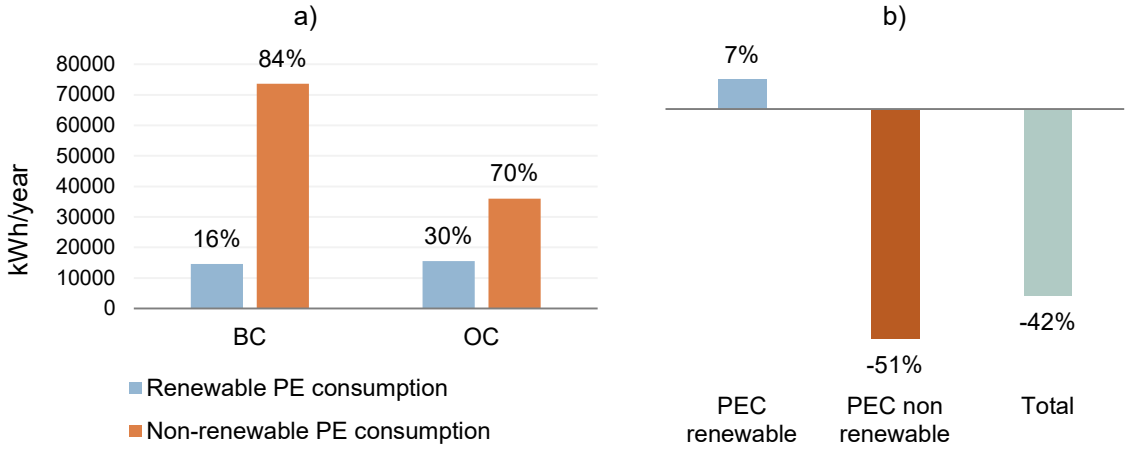

Fig. 20. On the left (a), the net PE consumption in BC and OC models is shown and the percentage over the total PE is also indicated. On the right (b), the percentage deviation in PE consumption of OC with respect to the BC scenario is shown. Renewable and non-renewable shares are represented separately.

The drastic reduction achieved in PE use, illustrated in these results, would bring the building very close to the NEC upper limits for total and non-renewable PE consumption for non-listed refurbished buildings in climate zone B4. However, total PE still deviates by 23% and non-renewable PE deviates by 26% above the mandatory limits (Fig. 21).

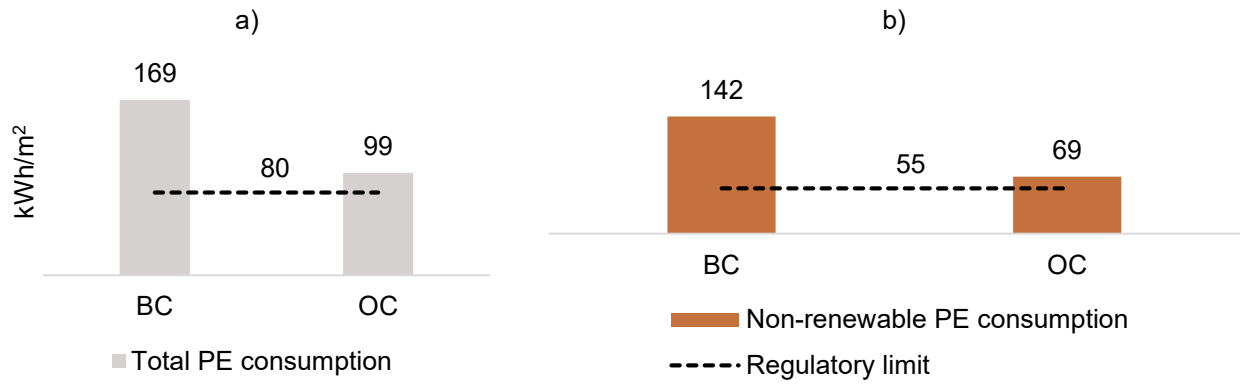

Fig. 21. Annual PE consumed per unit area in the BC and OC models compared to the NEC regulatory limits. On the left (a) the total amount and on the right (b) the non-renewable share.

6. Conclusions.

Historic town centres should not be excluded from the ambitious decarbonization plans for cities since the use of their housing stock, which constitutes theirs most abundant building type, following contemporary comfort and environmental standards, represents the most effective tool for conservation. Combining conservation, comfort, and energy efficiency goals is a complex task and residential historic buildings present specific constraints for fossil energy reduction. However, these do not prevent them from being retrofitted following highly demanding energy standards to bring them very close to NZEB. Specific envelope-related actions in combination with highly efficient technologies for ventilation and thermal energy supply, - based on hybrid technologies that integrate RESs into the public electricity grid -, have a huge potential to bring the energy performance of the Mediterranean historic housing very close to newly built or refurbished non-listed buildings.

This is the case of the case-study building analysed here, which is located in a conservation area that is one of the largest in Europe and has been granted the highest level of protection in Spain. Its renovation strategy was designed to address environmental, health and conservation demands, the interactions of which were also considered. Environmental demands pursue the reduction in final and primary energy use in order to reduce CO_2 emissions and the pollution caused by the building. Health demands aim to prevent thermal discomfort in the dwellings, enhancing indoor air quality while conservation demands have to do with the preservation of the material integrity and authenticity of the façades and with the need to avoid visual pollution. Climate conditions of 2017 were adopted for this research. As stated in Section 2, in that

year daily maximum temperatures were considerably higher than those of the historic records, especially in summer. However, these can be assumed for the near future, as they seem to reflect the official climate projections.

Our results show that (1) the proposed retrofit plan is capable of reducing the energy demand by 10%, while improving thermal comfort and indoor air quality in the dwellings, (2) the energy produced on site would fully cover the thermal needs of the building, (3) the final and primary energy consumption are reduced by 23% and 42% respectively and (4) the fossil-fuel energy consumption is reduced by 51%, saving a considerable amount of CO_2 emissions to the atmosphere. This significant improvement over the initial energy status, where primary energy consumption doubled the mandatory limit for refurbished non-listed buildings, was achieved while complying with the heritage protection rules (only 23% of the external wall surface was thermally insulated) and despite the fact that refrigeration was simulated for longer periods of time and a new mechanical ventilation system operated in a continuous mode. Within the set of improvement measures, the role of the hybrid system proposed, a highly efficient heat pump working in parallel with a common electric water heater, is primarily responsible for such enhancement and represents a feasible solution for most residential heritage buildings in Mediterranean historic cities.

However, according to the thresholds established in the national regulation, the case study cannot yet be considered a NZEB. Auxiliary renewable-based support technologies, such as PV or geothermal, would complete the task. PV could supply energy to the fans and pumps of the heat pump, which are large electricity consumers (they account for 26% of the global thermal final energy consumed annually) and geothermal heat-exchangers could save energy by reducing the inlet-outlet temperature gap, but are not always possible due to space restrictions or archaeological and landscape protection rules. This fact stresses the need to accelerate the decarbonization of the national electricity mix.

Our research analyses a case-study building emblematic of the conservation areas of many historic city centres in the Spanish Mediterranean region. The morphological and constructive heterogeneity of heritage housing stocks would nevertheless require a sufficiently representative sample to be analysed on a case-by-case basis. Pilot actions would help; they should include the monitoring of the post-retrofit status to accurately check the active systems' performance in actual climate and operational conditions, as well as its interaction with the residents' behaviour and the passive measures implemented in the buildings.

REFERENCES

[1] European Parliament, Directive 2012/27/EU of the European Parliament and of the Council, Off. J. Eur. Union Dir. (2012) 1–56. https://doi.org/10.3000/19770677.L_2012.315.eng.

[2] 2030 Climate Target Plan | Climate Action, (n.d.). https://ec.europa.eu/clima/policies/eu-climate-action/2030_ctp_en (accessed April 9, 2021).

[3] UNESCO World Heritage Centre, Recommendation on the Historic Urban Landscape, (2011). https://whc.unesco.org/en/hul/ (accessed February 18, 2019).

[4] ICOMOS, The Valletta Principles for the Safeguarding and Management of Historic Cities, Towns and Urban Areas, 2011. https://www.icomos.org/Paris2011/GA2011_CIVVIH_text_EN_FR_final_20120110.pdf.

[5] ICOMOS, Statement on the Adoption of the UN Sustainable Development Goals, n.d. www.icomos.org (accessed June 19, 2019).

[6] Intelligent Energy Europe. Energy EU Commission, NEW4OLD. New energy for old buildings., (n.d.). https://ec.europa.eu/energy/intelligent/projects/en/projects/new4old (accessed June 19, 2019).

[7] CARTIF Technology Centre, RENERPATH, (n.d.). https://www.cartif.com//en/international-projects/european/interreg/item/989-renerpath.html (accessed June 19, 2019).

[8] EU Intelligent Energy Europe. Energy EU Comission., 3encult. Efficient Energy for EU Cultural Heritage., 2010-2014. (n.d.). http://www.3encult.eu/en/project/welcome/default.html (accessed March 11, 2019).

[9] Interreg Europe, VIOLET. Preserve traditional buildings through energy reduction, (n.d.). https://www.interregeurope.eu/violet/ (accessed June 19, 2019).

[10] EFFESUS. Energy Efficiency for EU Historic Districts' Sustainability., 2012-2016. (n.d.). https://www.effesus.eu/.

[11] A.L. Webb, Energy retrofits in historic and traditional buildings: A review of problems and methods, Renew. Sustain. Energy Rev. 77 (2017) 748–759. https://doi.org/10.1016/j.rser.2017.01.145.

[12] R.A. Greta, C. Marta, S. Massimiliano, G. Laura, D. Pietromaria, Planning energy retrofit on historic building stocks: A score-driven decision support system, Energy Build. (2020) 110066. https://doi.org/10.1016/j.enbuild.2020.110066.

[13] F. Rosso, V. Ciancio, J. Dell'Olmo, F. Salata, Multi-objective optimization of building retrofit in the Mediterranean climate by means of genetic algorithm application, Energy Build. 216 (2020) 109945. https://doi.org/10.1016/j.enbuild.2020.109945.

[14] P.M. Congedo, C. Baglivo, S. Bonuso, D. D'Agostino, Numerical and experimental analysis of the energy performance of an air-source heat pump (ASHP) coupled with a horizontal earth-to-air heat exchanger (EAHX) in different climates, Geothermics. 87 (2020) 101845. https://doi.org/10.1016/j.geothermics.2020.101845.

[15] C. Baglivo, P.M. Congedo, D. Laforgia, Air cooled heat pump coupled with Horizontal Air-Ground Heat Exchanger (HAGHE) for Zero Energy Buildings in the Mediterranean climate, Energy Procedia. 140 (2017) 2–12. https://doi.org/10.1016/j.egypro.2017.11.118.

[16] EU Building Stock Observatory | Energy, (n.d.). https://ec.europa.eu/energy/topics/energy-efficiency/energy-efficient-buildings/eu-bso_en (accessed April 8, 2021).

[17] B. von Retteberg, I. Rodriguez-Maribona, Deliverable D1.1. European building and urban stock data collection. EU Project EFFESUS: Energy Efficeincy for EU Historic Districts Sustainability., 2013.

[18] Ministerio de Fomento del Gobierno de España., Observatorio de vivienda y suelo. Parque edificatorio., 2014.

[19] C.M. Muñoz González, A.L. León Rodríguez, R. Suárez Medina, J. Ruiz Jaramillo, Effects of future climate change on the preservation of artworks, thermal comfort and energy consumption in historic buildings, Appl. Energy. 276 (2020) 115483. https://doi.org/10.1016/j.apenergy.2020.115483.

[20] G.B.A. Coelho, H. Entradas Silva, F.M.A. Henriques, Impact of climate change in cultural heritage: from energy consumption to artefacts' conservation and building rehabilitation, Energy Build. 224 (2020). https://doi.org/10.1016/j.enbuild.2020.110250.

[21] A.A. Hamid, D. Johansson, H. Bagge, Ventilation measures for heritage office buildings in temperate climate for improvement of energy performance and IEQ, Energy Build. (2020) 109822. https://doi.org/10.1016/j.enbuild.2020.109822.

[22] N. Aste, R.S. Adhikari, M. Buzzetti, S. Della Torre, C. Del Pero, H.E. Huerto C, F. Leonforte, Microclimatic monitoring of the Duomo (Milan Cathedral): Risks-based analysis for the conservation of its cultural heritage, Build. Environ. 148 (2019) 240–257. https://doi.org/10.1016/j.buildenv.2018.11.015.

[23] L.F. Cabeza, A. De Gracia, A.L. Pisello, Integration of renewable technologies in historical and heritage buildings: A review, Energy Build. 177 (2018) 96–111. https://doi.org/10.1016/j.enbuild.2018.07.058.

[24] A. Egusquiza, S. Ginestet, J.C. Espada, I. Flores-Abascal, C. Garcia-Gafaro, C. Giraldo-Soto, S. Claude, G. Escadeillas, Co-creation of local eco-rehabilitation strategies for energy improvement of historic urban areas, Renew. Sustain. Energy Rev. 135 (2021) 110332. https://doi.org/10.1016/j.rser.2020.110332.

[25] V. Sugár, A. Talamon, A. Horkai, M. Kita, Energy saving retrofit in a heritage district: The case of the Budapest, J. Build. Eng. 27 (2020) 100982. https://doi.org/10.1016/j.jobe.2019.100982.

[26] A. Perez-Garcia, A.P. Guardiola, F. Gómez-Martínez, A. Guardiola-Víllora, Energy-saving potential of large housing stocks of listed buildings, case study: l'Eixample of Valencia, Sustain. Cities Soc. 42 (2018) 59–81. https://doi.org/10.1016/J.SCS.2018.06.018.

[27] M. Etxebarria Mallea, L. Etxepare Igiñiz, M. de Luxán García de Diego, Passive hygrothermal behaviour and indoor comfort concerning the construction evolution of the traditional Basque architectural model. Lea valley case study, Build. Environ. 143 (2018) 496–512. https://doi.org/10.1016/J.BUILDENV.2018.06.041.

[28] T. Blázquez, S. Ferrari, R. Suárez, J.J. Sendra, Adaptive approach-based assessment of a heritage residential

complex in southern Spain for improving comfort and energy efficiency through passive strategies: A study based on a monitored flat, Energy. 181 (2019) 504–520. https://doi.org/10.1016/j.energy.2019.05.160.

[29] European Parliament, Directive EU 2018/844 of the European parliament and of the council amending Directive 2010/31/EU on the energy performance of buildings and Directive 2012/27/EU on energy efficiency., 2018.

[30] IDAE (Instituto para la Diversificación y Ahorro de Energía), Project Sech-Spahousec, Analysis of the Energetic Consumption of the Residential Sector in Spain, 2016. www.idae.es.

[31] J. Fernández-Agüera, S. Domínguez, C. Alonso, F. Martín-Consuegra, Thermal comfort and indoor air quality in low-income housing in Spain: the influence of airtightness and occupant behaviour., Energy Build. (2019). https://doi.org/10.1016/j.enbuild.2019.06.052.

[32] L.J. Underhill, C.W. Milando, J.I. Levy, W.S. Dols, K. Sharon, M.P. Fabian, Simulation of indoor and outdoor air quality and health impacts following installation of energy-efficient retrofits in a multifamily housing unit, Build. Environ. (2019) 106507. https://doi.org/10.1016/j.buildenv.2019.106507.

[33] M. Ortiz, L. Itard, P.M. Bluyssen, Indoor environmental quality related risk factors with energy-efficient retrofitting of housing: A literature review, Energy Build. 221 (2020) 110102. https://doi.org/10.1016/j.enbuild.2020.110102.

[34] I. Theodoridou, M. Karteris, G. Mallinis, A.M. Papadopoulos, M. Hegger, Assessment of retrofitting measures and solar systems' potential in urban areas using Geographical Information Systems: Application to a Mediterranean city, Renew. Sustain. Energy Rev. 16 (2012) 6239–6261. https://doi.org/10.1016/j.rser.2012.03.075.

[35] Renewable Power – Analysis - IEA, (n.d.). https://www.iea.org/reports/renewable-power (accessed March 1, 2021).

[36] Red Eléctrica de España (REE), (n.d.). https://www.ree.es/es/datos/generacion/evolucion-renovable-no-renovable (accessed April 16, 2021).

[37] S. Nižetić, A.M. Papadopoulos, G.M. Tina, M. Rosa-Clot, Hybrid energy scenarios for residential applications based on the heat pump split air-conditioning units for operation in the Mediterranean climate conditions, Energy Build. 140 (2017) 110–120. https://doi.org/10.1016/j.enbuild.2017.01.064.

[38] R. Stasi, S. Liuzzi, S. Paterno, F. Ruggiero, P. Stefanizzi, A. Stragapede, Combining bioclimatic strategies with efficient HVAC plants to reach nearly-zero energy building goals in Mediterranean climate, Sustain. Cities Soc. 63 (2020) 102479. https://doi.org/10.1016/j.scs.2020.102479.

[39] A.S. Gaur, D.Z. Fitiwi, J. Curtis, Heat pumps and our low-carbon future: A comprehensive review, Energy Res. Soc. Sci. 71 (2021) 101764. https://doi.org/10.1016/j.erss.2020.101764.

[40] F. Neirotti, M. Noussan, M. Simonetti, Towards the electrification of buildings heating - Real heat pumps electricity mixes based on high resolution operational profiles, Energy. 195 (2020) 116974. https://doi.org/10.1016/j.energy.2020.116974.

[41] M. Jarre, M. Noussan, M. Simonetti, Primary energy consumption of heat pumps in high renewable share electricity mixes, Energy Convers. Manag. 171 (2018) 1339–1351. https://doi.org/10.1016/j.enconman.2018.06.067.

[42] G. Bagarella, R. Lazzarin, M. Noro, Annual simulation, energy and economic analysis of hybrid heat pump systems for residential buildings, Appl. Therm. Eng. 99 (2016) 485–494. https://doi.org/10.1016/j.applthermaleng.2016.01.089.

[43] M. Jarre, M. Noussan, A. Poggio, M. Simonetti, Opportunities for heat pumps adoption in existing buildings: Real-data analysis and numerical simulation, in: Energy Procedia, Elsevier Ltd, 2017: pp. 499–507. https://doi.org/10.1016/j.egypro.2017.09.608.

[44] I. Sarbu, C. Sebarchievici, Chapter 4. Types of Compressors and Heat Pumps, in: I. Sarbu, C. Sebarchievici (Eds.), Ground-Source Heat Pumps. Fundam. Exp. Appl., Elsevier, 2016: pp. 47–70. https://doi.org/10.1016/b978-0-12-804220-5.00004-7.

[45] K. Rice, B. Shen, J. Munk, M. Ally, V. Baxter, D.S. Engineers, Development of a Variable-Speed Residential Air-Source Integrated Heat Pump, in: 11thIEA Heat Pump Conf. 2014, May 12-16 2014, Montréal Canada., 2014: pp. 1–12.

[46] European Parliament, Guidelines for Member States on calculating renewable energy from heat pumps from different heat pump technologies pursuant to Article 5 of Directive 2009/28/EC, Off. J. Eur. Union. (2013) 27–35.

[47] CEN/TC 113, EN 14825:2018. Air conditioners, liquid chilling packages and heat pumps, with electrically driven compressors, for space heating and cooling. Testing and rating at part load conditions and calculation of seasonal performance., 2018.

[48] K. Klein, K. Huchtemann, D. Müller, Numerical study on hybrid heat pump systems in existing buildings, Energy Build. 69 (2014) 193–201. https://doi.org/10.1016/j.enbuild.2013.10.032.

[49] V. Bianco, F. Scarpa, L.A. Tagliafico, Estimation of primary energy savings by using heat pumps for heating purposes in the residential sector, Appl. Therm. Eng. 114 (2017) 938–947. https://doi.org/10.1016/j.applthermaleng.2016.12.058.

[50] C. Naldi, E. Zanchini, Dynamic simulation during summer of a reversible multi-function heat pump with condensation-heat recovery, Appl. Therm. Eng. 116 (2017) 126–133. https://doi.org/10.1016/j.applthermaleng.2017.01.066.

[51] G. Lo Basso, F. Rosa, D. Astiaso Garcia, F. Cumo, Hybrid systems adoption for lowering historic buildings PFEC (primary fossil energy consumption) - A comparative energy analysis, Renew. Energy. 117 (2018) 414–433. https://doi.org/10.1016/j.renene.2017.10.099.

[52] B. Torregrosa-Jaime, B. González, P.J. Martínez, G. Payá-Ballester, Analysis of the operation of an aerothermal heat pump in a residential building using building information modelling, Energies. 11 (2018). https://doi.org/10.3390/en11071642.

[53] R. Caro-Martínez, J.J. Sendra, Implementation of urban building energy modeling in historic districts. Seville as case-study, Int. J. Sustain. Dev. Plan. 13 (2018). https://doi.org/10.2495/SDP-V13-N4-528-540.

[54] Gerencia de Urbanismo del Ayuntamiento de Sevilla, Infraestructura de datos espaciales de Sevilla (ide.SEVILLA), (n.d.). https://sig.urbanismosevilla.org/InicioIDE.aspx (accessed February 11, 2019).

[55] M.C. Peel, B.L. Finlayson, T.A. McMahon, Updated world map of the Köppen-Geiger climate classification, Hydrol. Earth Syst. Sci. 11 (2007) 1633–1644. https://doi.org/10.5194/hess-11-1633-2007.

[56] Gobierno de España, AEMET (Agencia Estatal de Meteorología), (n.d.). http://www.aemet.es/es/portada (accessed February 10, 2019).

[57] C.M. Calama-González, R. Suárez, Á.L. León-Rodríguez, S. Domínguez-Amarillo, Evaluation of thermal comfort conditions in retrofitted facades using test cells and considering overheating scenarios in a mediterranean climate, Energies. 11 (2018). https://doi.org/10.3390/en11040788.

[58] European Environment Agency (EEA), Climate change, impacts and vulnerability in Europe 2016., 2017. https://www.eea.europa.eu/publications/climate-change-impacts-and-vulnerability-2016 (accessed January 21, 2020).

[59] V. Fernández Salinas, VIVIENDA MODESTA Y PATRIMONIO CULTURAL: LOS CORRALES Y PATIOS DE VECINDAD EN EL CONJUNTO HISTÓRICO DE SEVILLA, Scr. Nov. VII (2003). https://revistes.ub.edu/index.php/ScriptaNova/article/view/709/686.

[60] Ley 14/2007 del Patrimonio Histórico de Andalucía., 2012.

[61] Ministerio de Fomento del Gobierno de España, Código Técnico de la Edificación. Documento Básico Ahorro de Energía HE0. Limitación del consumo energético., 2019. https://www.codigotecnico.org/index.php/menu-ahorro-energia.html%0D.

[62] U.S. Department of Energy, Energy Plus, (n.d.). https://energyplus.net/ (accessed February 10, 2019).

[63] Department of Energy, (n.d.). https://www.energy.gov/ (accessed March 19, 2021).

[64] R. Caro, J.J. Sendra, Evaluation of indoor environment and energy performance of dwellings in heritage buildings. The case of hot summers in historic cities in Mediterranean Europe, Sustain. Cities Soc. 52 (2020) 101798. https://doi.org/10.1016/j.scs.2019.101798.

[65] R. Caro, J.J. Sendra, Are the dwellings of historic Mediterranean cities cold in winter? A field assessment on their indoor environment and energy performance, Energy Build. 230 (2021) 110567. https://doi.org/10.1016/j.enbuild.2020.110567.

[66] U.S. Department of energy, M & V Guidelines : Measurement and Verification for Performance-Based Contracts Version 4.0., 2015. https://doi.org/10.1039/c8ew00545a.

[67] Á.L. León, S. Domínguez, M.A. Campano, C. Ramírez-Balas, Reducing the Energy Demand of Multi-Dwelling Units in a Mediterranean Climate Using Solar Protection Elements, 5 (2012) 3398–3424. https://doi.org/10.3390/en5093398.

[68] CTN100 Climatización, UNE-EN-16798-1. Eficiencia energética de los edificios., 2020.

[69] E. y T.G. de E. Ministerio de Industria, Factores de emisión de CO2 y coeficientes de paso a energía primaria de diferentes fuentes de energía final consumidas en el sector de edificios en España., 2016.

[70] CEN/TC 33, EN 12207:2016. Windows and doors. Air permeability. Classification., n.d.

[71] Ministerio de Fomento del Gobierno de España, Código Técnico de la Edificación. Documento Básico HS Salubridad, 2017.

[72] B. Shen, J. New, V. Baxter, Air source integrated heat pump simulation model for EnergyPlus, Energy Build. 156 (2017) 197–206. https://doi.org/10.1016/j.enbuild.2017.09.064.

[73] Ministerio de Fomento del Gobierno de España., Código Técnico de la Edificación. Docuemnto Básico HE1. Condiciones para el control de la demanda energética., 2019.

[74] U.S. Department of energy. Energy Efficiency & Renewable Energy., M&V Guidelines : Measurement and Verification for Performance-Based Contracts. Version 4.0, 2015.

[75] D.I. Kolaitis, E. Malliotakis, D.A. Kontogeorgos, I. Mandilaras, D.I. Katsourinis, M.A. Founti, Comparative assessment of internal and external thermal insulation systems for energy efficient retrofitting of residential buildings, Energy Build. 64 (2013) 123–131. https://doi.org/10.1016/j.enbuild.2013.04.004.

[76] A. Figueiredo, J. Figueira, R. Vicente, R. Maio, Thermal comfort and energy performance: Sensitivity analysis to apply the Passive House concept to the Portuguese climate., Build. Environ. 103 (2016) 276–288. https://doi.org/10.1016/j.buildenv.2016.03.031.